Nanoscale

ROYAL SOCIETY OF CHEMISTRY

REVIEW

View Article Online
View Journal | View Issue

Cite this: *Nanoscale*, 2025, **17**, 7617

Recent advances in functional lipid-based nanomedicines as drug carriers for organ-specific delivery

Yeochan Yun,†[a] Jeongmin An,†[a] Hyun Joong Kim,†[a] Hye Kyu Choi[b] and Hyeon-Yeol Cho *[a]

Lipid-based nanoparticles have emerged as promising drug delivery systems for a wide range of therapeutic agents, including plasmids, mRNA, and proteins. However, these nanoparticles still encounter various challenges in drug delivery, including drug leakage, poor solubility, and inadequate target specificity. In this comprehensive review, we present an in-depth investigation of four distinct drug delivery methods: liposomes, lipid nanoparticle formulations, solid lipid nanoparticles, and nanoemulsions. Moreover, we explore recent advances in lipid-based nanomedicines (LBNs) for organ-specific delivery, employing ligand-functionalized particles that specifically target receptors in desired organs. Through this strategy, LBNs enable direct and efficient drug delivery to the intended organs, leading to superior DNA or mRNA expression outcomes compared to conventional approaches. Importantly, the development of novel ligands and their judicious combination holds promise for minimizing the side effects associated with nonspecific drug delivery. By leveraging the unique properties of lipid-based nanoparticles and optimizing their design, researchers can overcome the limitations associated with current drug delivery systems. In this review, we aim to provide valuable insights into the advancements, challenges, and future directions of lipid-based nanoparticles in the field of drug delivery, paving the way for enhanced therapeutic strategies with improved efficacy and reduced adverse effects.

Received 14th November 2024,
Accepted 24th February 2025

DOI: 10.1039/d4nr04778h

rsc.li/nanoscale

Introduction

Advancements in pharmaceutical research have led to the development of a diverse range of drugs tailored to combat specific diseases.[1] While these efforts have yielded significant clinical success, the delivery of certain drugs, especially those with poor water solubility or lipophilic properties, remains a critical challenge. For instance, over 40% of approved drugs exhibit low water solubility, necessitating their dilution in amphiphilic solvents for effective administration.[2] Conversely, hydrophilic drugs often suffer from suboptimal loading efficiencies in conventional drug carriers, highlighting the need for novel delivery platforms.[3] These limitations have spurred intensive research into lipid-based nanomedicines (LBNs), which have demonstrated remarkable potential as versatile drug delivery systems.[4] These LBNs have emerged as promising drug delivery platforms due to their remarkable biocompatibility, high drug-loading capacity, and ability to encapsulate both hydrophobic and hydrophilic drugs. Continued drug delivery studies on LBNs aim to minimize the occurrence of toxic side effects while maximizing the pharmacological effects of the drugs.[5,6]

The field of drug delivery research has undergone significant advancements, particularly in the development of nanoparticle-based systems, which have demonstrated remarkable improvements in targeted drug delivery by modifying physicochemical properties such as size and charge to enhance organ-specific delivery efficiency.[7] Despite these promising developments, nanoparticles still face biological barriers that hinder their precision, including nonspecific accumulation caused by the enhanced permeability and retention (EPR) effect, which, although widely studied as a passive targeting mechanism, has shown limited efficacy in clinical contexts.[8–12] Lipid nanoparticles (LNPs), a prominent subclass of LBNs, have emerged as particularly promising candidates for therapeutic applications due to their excellent biocompatibility, tunable physicochemical properties, and ability to facilitate organ-specific drug delivery. Recent studies have focused on improving LNP performance through surface functionalization with ligands and polymers, which enhance circulation time, cellular

[a]*Department of Bio & Fermentation Convergence Technology, Kookmin University, Seoul 02707, Republic of Korea. E-mail: chohy@kookmin.ac.kr*
[b]*Department of Chemistry and Chemical Biology, Rutgers University, the State University of New Jersey, 123 Bevier Road, Piscataway, New Jersey 08854, USA*
†These authors contributed equally.

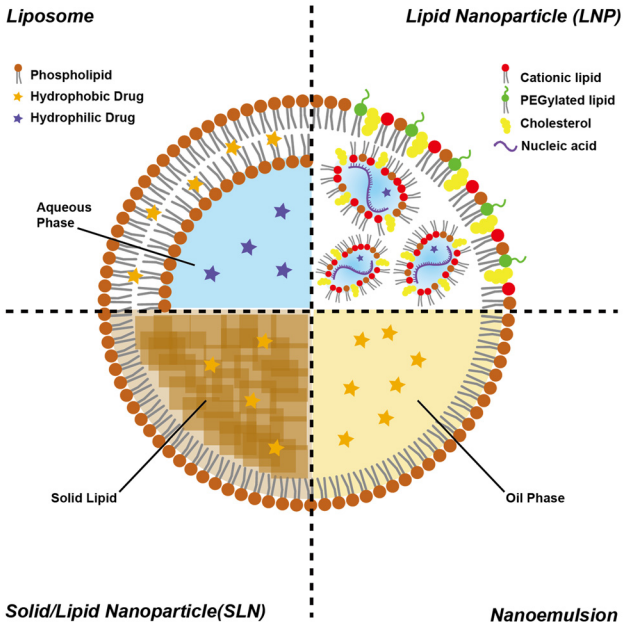

Fig. 1 Illustration of versatile lipid-based drug carriers for drug delivery.

uptake, and targeting capabilities.[13,14] To overcome the remaining challenges, researchers have developed diverse targeting strategies, including small molecules, peptides, antibodies, and cell-based approaches, to further improve the precision and therapeutic outcomes of these delivery systems.[15]

This review highlights the transformative potential of lipid-based nanomedicines in organ-specific drug delivery by synthesizing the latest advancements in functionalization strategies. By focusing on the development of liposomes, LNPs, solid lipid nanoparticles (SLNs), and nanoemulsions, this review underscores the versatility of these carriers in overcoming current limitations in drug delivery (Fig. 1). Furthermore, this work explores innovative engineering approaches to improve drug stability, enhance biodistribution, and reduce adverse side effects.

In this context, we provide a comprehensive overview of recent advancements in lipid-based nanomedicines, with an emphasis on their applications in treating diseases affecting specific organs, such as the liver, lungs, brain, pancreas, and spleen. Through this review, we aim to equip researchers with the insights necessary to advance drug delivery systems and foster the development of novel therapeutic strategies, ultimately improving patient outcomes across a range of disease areas.

Types of functional lipid-based nanocarriers for drug delivery

The selection of nanocarrier formulations, including liposomes, LNPs, SLNs, and nanoemulsions, is significantly influenced by the type of payload, *i.e.* hydrophobic drugs, hydrophilic drugs, and nucleic acids.[16] Hydrophobic drugs, for example, are well-suited for liposomes and SLNs due to their lipid-rich core, which enhances encapsulation efficiency and stability, as demonstrated in the delivery of poorly water-soluble chemotherapeutics.[17] In contrast, hydrophilic drugs benefit from nanoemulsions and LNPs with aqueous cores, which improve solubility and bioavailability, particularly for small-molecule hydrophilic compounds.[18] Finally, nucleic acids, such as mRNA or siRNA, require ionizable lipids in LNPs to facilitate efficient encapsulation, endosomal escape, and cytosolic delivery, making them ideal for gene therapy and RNA-based therapeutics.[19] The payload-specific requirements emphasized in this context underscore the importance of matching formulation properties with the physicochemical characteristics of the payload, thereby optimizing delivery efficiency and therapeutic outcomes. The following section will delve into the detailed formulation characteristics of each nanocarrier.

Liposomes

Liposomes, which are composed of lipid bilayers that can encapsulate both hydrophobic and hydrophilic drugs, are a type of nanocarrier widely used for drug delivery purposes. The liposome structure, like biological membranes, can stabilize drug compounds against external degradation and enable their absorption and delivery to cells and tissues.[20] Liposomes are primarily composed of lipids (*e.g.*, sphingolipids, phospholipids, and glycolipids), sterols (*e.g.*, desmosterol and cholesterol), polysaccharides (*e.g.*, chitosan and hyaluronic acid [HA]), and surfactants (*e.g.*, polysorbate 80 and Span 80) (Fig. 2A).[21]

During the synthesis of liposomes *via* thin film formation, a freeze–thaw protocol is employed to enhance the entrapment efficiency of lipophilic drugs.[22] First, the lipophilic drug and amphiphilic molecules are hydrated and mixed with an organic solvent before transferring the mixture to a round-bottom flask and evaporating the solvent using a rotary evaporator under vacuum to form a lipid layer (thin film), which includes the lipophilic drug. Subsequently, the lipid layer solution is sonicated at room temperature, frozen in liquid nitrogen, and then thawed at room temperature, resulting in the fusion of liposomes as the liposome solution melts. This cycle can be repeated up to 10 times to create large unilamellar vesicles (LUVs). The nano size of the vesicles can be acquired by sonication of the resulting solution at room temperature (Fig. 2B). The formed lipid bilayer contains hydrophobic drugs, while the middle layer accommodates hydrophilic drugs (Fig. 2C). Depending on the synthesis method, liposomes are typically synthesized in the range of approximately 100–200 nm (Fig. 2D).[23] Liposome structures are categorized based on their surface features, resulting in a reduction in nonspecific side effects and enabling a wide range of applications in drug administration.

As an example of liposomes synthesized using the freeze–thaw-thin-film hydration technique, liposome encapsulation of the iridium(III) complex Ir(bzq)2(PYIP) (Ir1, where bzq:

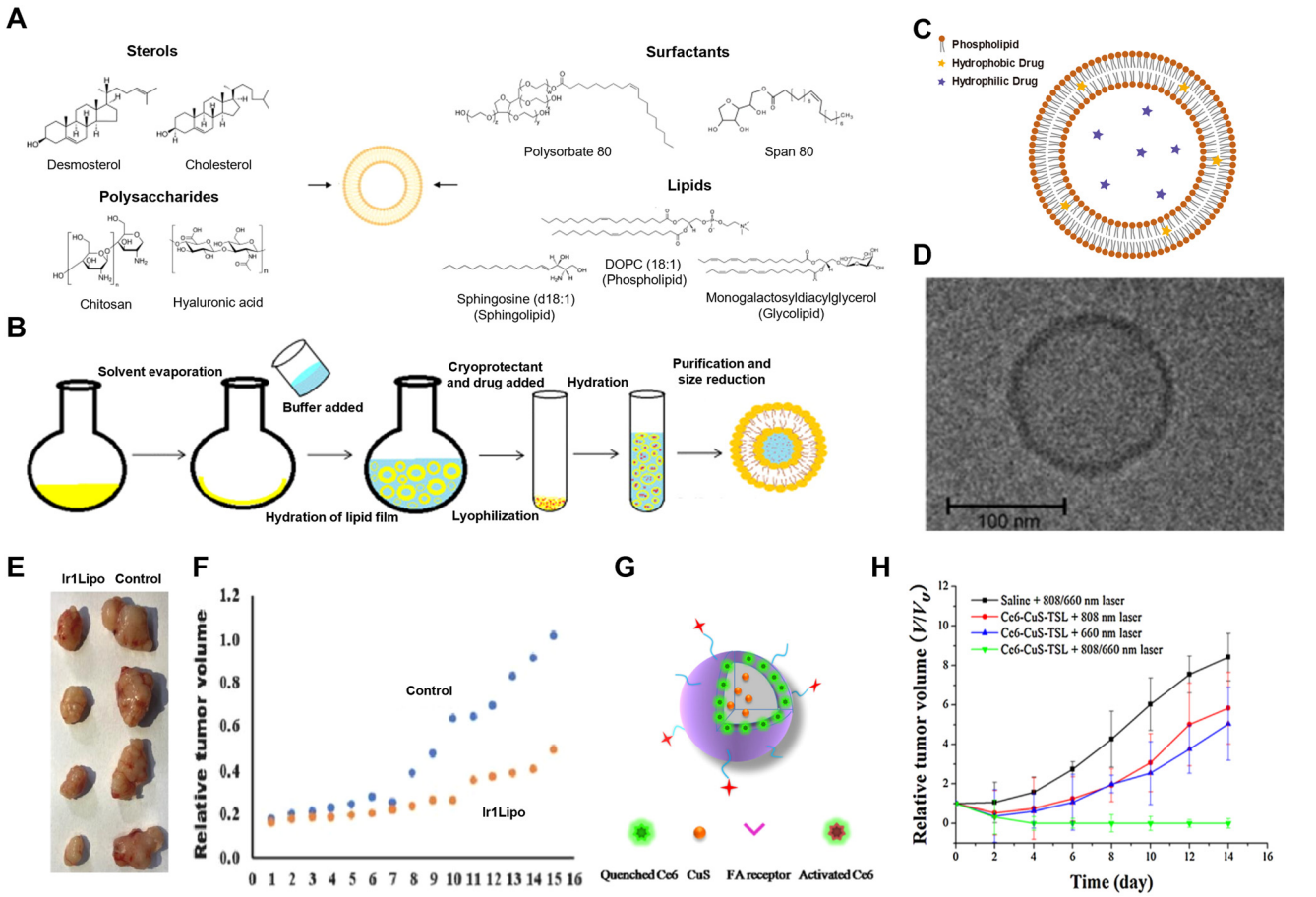

Fig. 2 Structure and synthesis of liposomes. (A) Four major chemical components required for liposome synthesis. Reproduced with permission from ref. 21. Copyright 2021, Elsevier. (B) Representative liposome synthesis method. Reproduced with permission from ref. 22. Copyright 2014, Elsevier. (C) Drug-loading location and structure of liposomes. (D) Cryo-TEM image of a liposome. Reproduced with permission from ref. 23. Copyright 2020, The Author(s). (E) Photographs of tumor treated with iridium(III)-complex liposome (Ir1Lipo), and (F) *in vivo* antitumor activity of Ir1Lipo. Reproduced with permission from ref. 24. Copyright 2021, Elsevier. (G) Liposomes modified by Ce6-CuS, and (H) relative tumor volume curves of various mouse groups following different indicated treatments. Reproduced with permission from ref. 25. Copyright 2016, Elsevier.

benzo[*h*]quinoline and PYIP: 2-(pyren-1-yl)-1*H*-imidazo[4,5-*f*][1,10]phenanthroline) has been used as a potent anticancer reagent.[24] These nanosized liposomes have a diameter of approximately 121.6 ± 2 nm, imparting easy penetration of cell membranes. Regarding *in vivo* antitumor activity, the results demonstrated a rapid increase in relative tumor volume on the eighth day for the blank group, whereas the group treated with the iridium(III) complex-liposome (Ir1Lipo; 1.8 mg kg^{-1}) exhibited a minimal change in tumor volume, suggesting that Ir1Lipo has an inhibitory effect (Fig. 2E and F).

Liposomes can also be engineered to generate photothermal effects for photodynamic therapy (PDT).[25] PDT relies on a photosensitizer to transfer photon energy to surrounding oxygen molecules, leading to the generation of reactive oxygen species (ROS), including singlet oxygen ($^1O_2$), upon irradiation, ultimately targeting and eliminating tumor cells. In this experiment, thermosensitive liposomes (TSLs) serve as a nanocarrier to enhance the solubility, stability, and biocompatibility of the photosensitizer chlorin e6 (Ce6) (Fig. 2G). Furthermore, copper sulfide (CuS) functions as a photothermal agent to induce heat release. *In vivo* testing revealed that the groups treated with Ce6-CuS-TSL (comprising photothermal therapy [PTT], PDT, and PTT/PDT) exhibited a noteworthy delay in tumor growth compared to the saline-treated group. Particularly, the combined PTT/PDT group displayed superior therapeutic efficacy compared to standalone PTT or PDT treatments, indicating a synergistic effect. Additionally, the combined PTT/PDT approach significantly extended the survival rate of mice, with a 14.29% survival rate up to 60 days. Conversely, the saline-, PTT-, and PDT-treated groups showed shorter median survival times (21, 29, and 40 days, respectively) (Fig. 2H).

Liposomes and LNPs are both lipid-based nanocarriers, but they differ in structural complexity and application. Liposomes are spherical vesicles composed of one or more phospholipid bilayers surrounding an aqueous core, whereas LNPs are more advanced lipid-based nanocarriers typically designed with a multi-component structure, including ionizable lipids, chole-

sterol, phospholipids, and PEG-lipids. These components work synergistically to encapsulate and deliver various payloads, including genetic materials such as mRNA and siRNA. The ionizable lipids in LNPs are particularly critical for nucleic acid delivery as they enable efficient endosomal escape, a feature not typically optimized in conventional liposomes.[26] More detailed information on LNPs is introduced in the next section.

Lipid nanoparticles (LNPs)

Liposomes have demonstrated remarkable efficacy as delivery vehicles for small-molecule drugs. In contrast, the successful encapsulation, delivery, and controlled release of macromolecular drugs present formidable challenges, impeding the attainment of sufficient drug delivery levels.[27] To overcome these limitations, novel LNPs have been developed as promising carriers capable of providing stable and efficient delivery of macromolecular and gene-based therapeutics,[28–30] with distinctive charge characteristics.

Traditional lipid nanoparticles (LNPs) are composed of four key lipid components, each serving an essential and complementary role to enable efficient drug delivery (Fig. 3A). Ionizable lipids are critical for encapsulating nucleic acids through electrostatic interactions at acidic pH and facilitating endosomal escape by disrupting the endosomal membrane after internalization. Amphiphilic lipids, such as phospholipids, contribute to the structural integrity of LNPs and promote fusion with cellular and endosomal membranes,

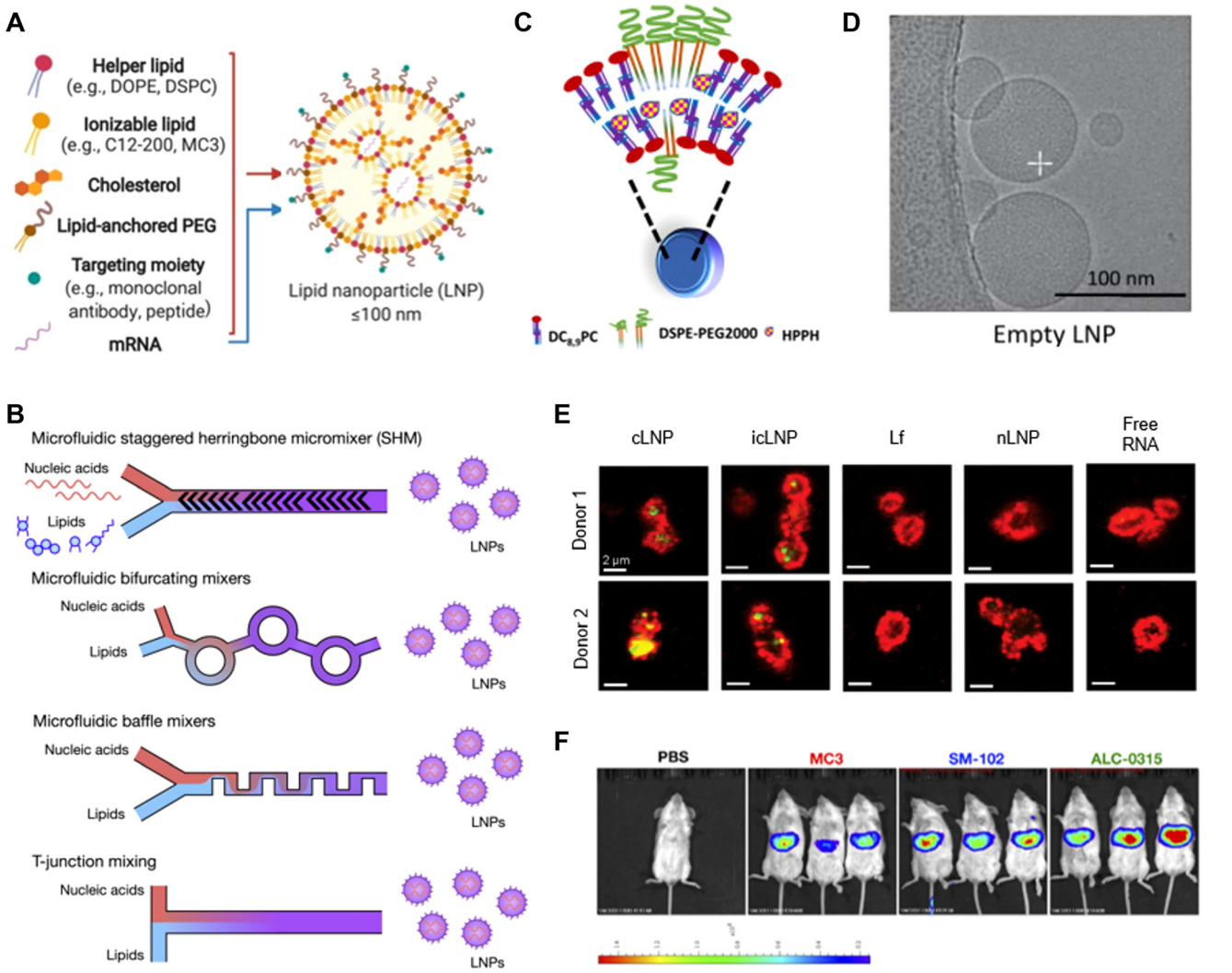

Fig. 3 Structure and synthesis of LNPs. (A) Schematic illustration of the components and structure of LNPs. Reprinted with permission from ref. 31. Copyright 2021, Elsevier. (B) Schematic illustration of microfluidic devices used in LNP synthesis. Reproduced with permission from ref. 36. Copyright 2021, Elsevier. (C) Schematic of drug loading into LNPs. Reprinted with permission from ref. 38. Copyright 2018, Elsevier. (D) Cryo-TEM images of empty LNPs. Reprinted with permission from ref. 39. Copyright 2022, The Author(s). (E) Confocal immunofluorescence microscopy of platelets (red) transfected with LNPs containing biotin-labelled RNA (green). Representative images from four separate donors are shown. Scale bars: 2 μm. Reproduced with permission from ref. 40. Copyright 2019, The Author(s). (F) Luciferase expression 6 h after injections of mRNA-loaded MC3-, SM-102-, and ALC-0315-based LNPs. Reproduced with permission from ref. 41. Copyright 2023, The Author(s).

enabling the release of the encapsulated cargo into the cytosol. Cholesterol enhances LNP stability by modulating membrane fluidity and packing, ensuring the structural robustness of the nanoparticles during systemic circulation. Poly(ethylene glycol) (PEG) lipids provide a steric barrier to reduce non-specific protein adsorption, thereby improving colloidal stability and minimizing clearance by the reticuloendothelial system (RES), which prolongs circulation time.[31] These lipid components work synergistically to confer the chemical and physical properties necessary for efficient drug delivery, from systemic stability and endocytosis to intracellular release and cytosolic delivery.[32]

LNPs are produced primarily through the microfluidic mixing method. Mixing of lipids in ethanol and drug-containing buffer creates an emulsion, and cholesterol and PEG help to maintain the structure, forming stable particles.[32,33] Increasing the flow rate of the buffer creates smaller particles and enhances cellular delivery efficiency, but an excessively fast rate can affect drug encapsulation (Fig. 3B). Thus, it is essential to identify an appropriate buffer flow rate for each drug.[34,35] The methods shown in Fig. 3B (staggered herringbone micromixer [SHM] devices, bifurcating mixing, baffle mixing, and T-junction mixing) are used to change the structure of the microfluidic mixing device to alter the flow rate.[36] Each method has its own merits. SHM devices show good efficiency in generating particles smaller than 100 nm. In bifurcating mixing, the encapsulation efficiency is over 90%. Baffle mixers can fine-tune particle size, and T-junction mixing has an efficiency suitable for large-scale production. Creating an LNP using a suitable device can improve the results.

LNPs can load both hydrophobic and hydrophilic drugs. The properties of phospholipids allow the creation of aqueous cores inside the particles. Hydrophilic drugs are loaded into the aqueous core through electrostatic interactions or reverse-evaporation vesicle (REV) methods. The outer layer of the hydrophilic core forms a lipophilic space due to the lipophilic tails of the lipids.[37] In this way, hydrophobic drugs become attached to the lipid tails during particle formation and are loaded into the lipophilic space. For example, LNPs developed using 1,2-dipalmitoyl-*sn-glycero*-3-phosphocholine (DPPC), which induces a stable vesicle structure, are suitable for delivering the hydrophobic PDT drug 2-[1-hexyloxyethyl]-2-devinyl pyropheophorbide-α (HPPH) (Fig. 3C).[38] Successful delivery is accomplished by capitalizing on the inherent ability of HPPH to bind selectively to DPPC cluster pockets. The strategic modification of PEGylated lipids in LNPs can enable efficient loading of hydrophobic drugs, facilitating targeted delivery, as evidenced by Cry-TEM images of the empty interior of LNPs (Fig. 3D).[38,39]

Efficient cell transfer of LNPs can be achieved using various types of lipids. As shown in Fig. 3E, the degree of expression of fluorescent messenger RNA (mRNA) delivered to the platelets changes depending on the type of lipid: LNPs containing a cationic lipid that remains positively charged at physiological pH (cLNPs), LNPs containing an ionizable cationic lipid that is neutral at physiological pH but becomes positively charged in acidic conditions (icLNPs), or LNPs lacking cationic lipids (nLNPs).[40] Treatment with cLNPs showed better effects than other types of LNPs, and it has been confirmed that icLNPs also became cationic under acid conditions. As described above, when the ionized lipid is changed, the degree of expression of fluorescent mRNA when administered by the intravenous (IV) route to mice.[41] These findings show that it is possible to increase the efficiency of the experiment by changing the ionized lipids to suit the target organ or cell (Fig. 3F).

Solid lipid nanoparticles (SLNs)

SLNs are characterized by a solid lipid matrix, which results in enhanced interparticle interactions and structural stability. Additionally, the presence of surfactants facilitates the formation of a hydrophilic layer on the particle surface, promoting electrostatic repulsion. These attributes confer SLNs a significant advantage in mitigating particle aggregation compared to LNPs, which possess a mixed solid–liquid lipid structure associated with weaker interparticle interactions and greater fluidity.[42] SLNs have a solid lipid core surrounded by a shell layer composed of phospholipids. The SLN core consists of lipids such as mono-, di-, and triglycerides, fatty acids, waxes, steroids, and other solid lipids.[43,44] The incorporation of these lipids enhances biocompatibility and increases resistance to drug release, allowing for precise control over drug delivery (Fig. 4A).[45]

Two conventional techniques have been used to synthesize SLNs: (1) hot homogenization and (2) high-pressure homogenization. Hot homogenization entails the fusion and emulsification of lipid materials through the use of a mixer and homogenizer,[46] whereas high-pressure homogenization involves the application of force to liquid substances by passing them through a narrow gap at high speed.[47] As a result, SLNs are formed with an average particle size ranging between 100 and 200 nm. These SLNs exhibit the capability to encapsulate both hydrophilic and hydrophobic drugs, rendering them suitable for efficient drug-loading purposes (Fig. 4B).[48–50]

The incorporation of hydrophilic drugs within SLNs can be facilitated by modifying PEG to directly link with drug molecules, enabling the hydrophilic drugs to be efficiently delivered through the bloodstream. Conversely, hydrophobic drugs can be dissolved or dispersed in lipid melts or integrated into the bulk lipid matrix during particle formation, allowing them to co-exist within the solid lipid core of SLNs. This versatile approach ensures effective encapsulation and delivery of both hydrophilic and hydrophobic drugs using SLNs as carriers.[47]

SLNs have been used to encapsulate and deliver hydrophobic drugs, such as rapamycin and docetaxel (DTX). Hydrophobic drugs, such as rifampicin and dapsone, can be loaded into the lipid core using lactonic sophorolipid and dispersed as SLNs by adding poloxamer, which assists with the generation of the particles (Fig. 4C and D). SLNs have the ability to release drugs at 37 °C (normal human body temperature). The resulting lactonic sophorolipid-SLNs have shown improved cellular delivery and exhibit excellent antimicrobial,

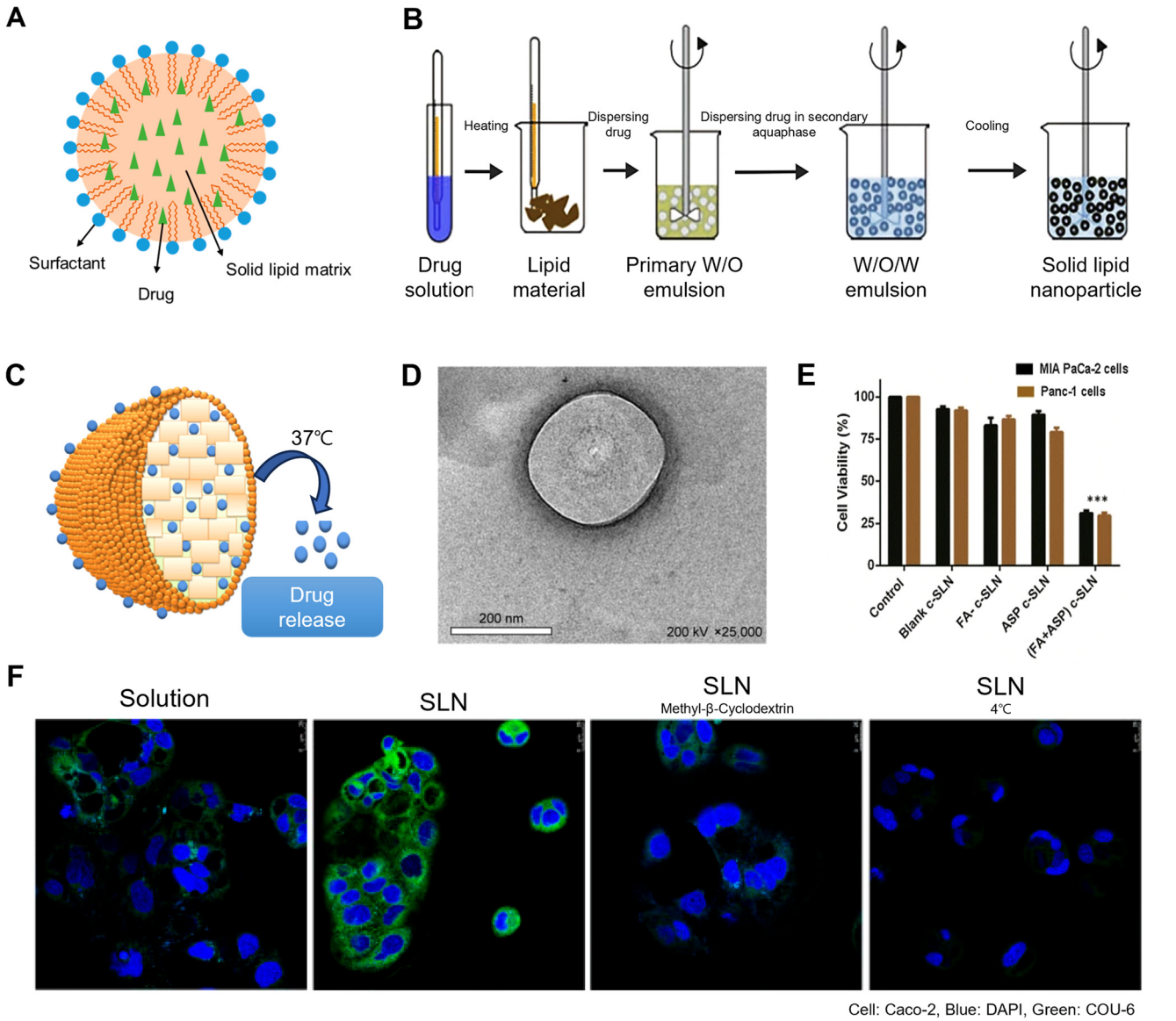

Fig. 4 Structure and synthesis of SLNs. (A) Components of SLNs. Reproduced with permission from ref. 45. Copyright 2020, MDPI. (B) Representative synthesis method of drug-loaded SLNs. Reproduced with permission from ref. 50. Copyright 2017, Elsevier. (C) Drug-loading location and drug release condition of SLNs. Reproduced with permission from ref. 51. Copyright 2018, American Chemical Society. (D) Cryo-TEM image of SLNs. Reproduced with permission from ref. 52. Copyright 2018, The Author(s). (E) Solid lipid nanoparticle (c-SLN) encapsulated FA + ASP combination. Reproduced with permission from ref. 53. Copyright 2015, The Author(s). (F) Confocal laser-laser optical microscopy of Caco-2 cells in four cases (Cou-6 suspension, transfer of Cou-6 loaded SLN, transfer of methyl-β-cyclodextrin and Cou-6 loaded SLN together, and transfer of Cou-6-loaded SLN cultured at 4 °C). 4′,6-Diamidino-2-phenylindol (DAPI, blue), fluorescent coumarin-6 (Cou-6, green). Reproduced with permission from ref. 54. Copyright 2020, MDPI.

antiviral, antifungal, anti-inflammatory, and anticancer activities.[51,52] SLNs can also load and deliver aspirin (ASP), an anti-inflammatory drug, and ferulic acid (FA), an antioxidant, simultaneously. In this regard, SLNs can be considered a useful drug carrier when two drugs must be used simultaneously for a disease. For example, it has been confirmed that treatment with ASP + FA-SLNs resulted in a reduction in pancreatic cancer cells of more than 45% compared to treatment with ASP-SLNs and FA-SLNs, respectively (Fig. 4E).[53]

Delivery of drugs through SLNs is a cell absorption method that is dependent on cholesterol and energy. To confirm whether SLNs can enhance intracellular delivery, a fluorescent microscopy experiment was performed using Caco-2 cells. Florescent dye coumarin 6 (Cou-6)-loaded SLNs with methyl-β-cyclodextrin inhibitors made intracellular infiltration using cholesterol impossible. Moreover, when Caco-2 cells cultured at 4 °C were treated with Cou-6-loaded SLNs, the cell absorption efficiency was low. Therefore, in the above two cases, it was confirmed that the fluorescence intensity was significantly

reduced compared to when Cou-6-loaded SLNs were easily delivered (Fig. 4F).[54]

Nanoemulsions/oleosomes

Through surface coating with PEG, LNPs can be functionalized with peptides, antibody molecules, or specific drug moieties to facilitate targeted drug delivery while mitigating the risk of myocarditis, a potential side effect induced by LNPs.[12] From this perspective, ionized lipid-based nanoemulsions represent an alternative material. A nanoemulsion is a type of emulsion with droplets ranging in diameter from 20 to 200 nm, which is much smaller in structure compared to conventional emulsions. A nanoemulsion is thermodynamically stable, meaning that it can remain dispersed without separation or aggregation for an extended period.[55] Due to their high biocompatibility and physical–chemical structural stability, nanoemulsions have been widely used in the fields of foods, cosmetics, pharmaceuticals, and chemical industries. Generally, nanoemulsions consist of an oil phase, a water phase, and an emulsifier and form either oil-in-water (o/w) or water-in-oil (w/o) emulsions, depending on the type of emulsifier (Fig. 5A).[56]

When a nanoemulsion is used as a drug carrier, it is mostly used as an o/w type.[57] The method for producing an o/w nanoemulsion involves preparing the aqueous phase by incorporating emulsifiers into distilled water. To illustrate, in one study, two combinations were used, both of which maintained a 70 : 30% w/w ratio. One combination involved the incorporation of maltodextrin (MD) with octenyl succinic anhydride (OSA)-modified starch capsule (MD-CAP), and the other combination used sodium caseinate (MD-SC). Mixtures (MD-CAP or MD-SC) were stirred magnetically. Subsequently, Tween 80 (1%, w/w) was added to the aqueous phase and stirred for a further 30 min. Then, the organic phase (1%, w/w), comprising lipophilic vitamin (A or E), was incorporated dropwise into the aqueous phase while it was homogenized using a homogenizer operating to obtain a coarse emulsion (o/w). Finally, to obtain the nanoemulsion, the coarse emulsion was homogenized by ultrasonication at 80% of the amplitude with a stainless-steel ultrasound probe (Fig. 5B).

Oleosomes are oil droplets surrounded by a sophisticated membrane consisting of a lipid monolayer and embedded oleosin proteins, forming a spherical structure with sufficient interfacial properties to stabilize o/w nanoemulsions. Oleosomes have been used in the cosmetics field and, more recently, for drug delivery applications due to their robustness in physiological conditions.[58] A highly functional oleosome capable of targeting and tracking was developed by using a recombinant protein consisting of immunoglobulin-binding protein LG fused to a green fluorescent protein (GFP-LG) to couple the oleosome to a HER2 antibody (specific to human breast carcinoma cells, SK-BR-3 cells) without chemical treatment-based conjugation (Fig. 5C). Atomic force microscopy (AFM) was performed to validate the structural integrity of the produced oleosomes. The stability of the oleosomes was evident from the uniform ellipsoidal structure of the phospholipid-(oleosin-hydrophilic domain linker-nanobody of GFP, OHNG) membrane in ambient conditions, displaying a diameter of 276 nm and a height of 5.9 nm (Fig. 5D and E). *In vivo* testing on mice confirmed that the oleosome selectively delivered drugs to the target cancer cells, and the oleosome which contained magnetic nanoparticles exhibited a killing efficiency of approximately 40% *via* magnetic hyperthermia in comparison to equivalent concentrations of the carmustine oleosome (Fig. 5F).

Another example of a nanoemulsion is the use of astaxanthin–α-tocopherol as a drug for wound healing (Fig. 5G).[59] In this experimental study, astaxanthin was loaded into nanostructured lipid carriers to synthesize nanoemulsions through two distinct methods, namely the spontaneous emulsification method (SENE) and the ultrasonication method (USNE), with the resulting nanoemulsion samples designated as SENE and USNE samples, respectively. Subsequently, the synthesized nanoemulsion containing astaxanthin–α-tocopherol was shown to promote wound closure in CT26 cells, as assessed by the *in vitro* scratch assay (also known as the monolayer wound assay). The nanoemulsion methods employed in this study include both SENE (a–c) and USNE (d–f) (Fig. 5H). Following cell adhesion, a noticeable reduction in wound size was observed as early as 6 h post-scratching. It is important to note that in long-term wound healing assays (>24 h), distinguishing between cell proliferation, changes in cell survival, and cell motility becomes challenging. The cells exhibited various migration patterns, including single-cell migration, migration as loosely connected populations, or collective migration as sheets of cells, particularly in the case of epithelial cells (Fig. 5H). Furthermore, in HeLa, CT26, and T24 cells, the rate of wound closure was significantly higher at a concentration of 25 mg mL^{-1} within 12 h compared to other concentrations, likely due to the presence of viable cells in the wounded tissue area (Fig. 5I). The synthesized nanoemulsion/oleosome can provide a versatile and effective drug delivery system with significant potential to advance cancer therapy.

Functionalization of LBNs for organ-specific delivery

Recently, receptor-targeting studies have been actively conducted,[60,61] in which the aforementioned LBNs are being used with ligands for target-specific delivery. Therefore, many scientists identified how LBNs could be targeted to each organ and used this mechanism to introduce the target-specific delivery system to each organ, including the liver, lung, pancreas, brain, and spleen, by functionalizing the ligands on the surface of LBNs (Fig. 6 and Table 1).

To achieve target-specific delivery, we aim to exploit ligand–receptor interactions by introducing ligand-functionalized LBNs on the surface. This approach is designed to enhance the specificity of delivery to the intended target. In addition, non-ligand-functionalized LBNs can also contribute to target-specific delivery by leveraging other mechanisms, such as

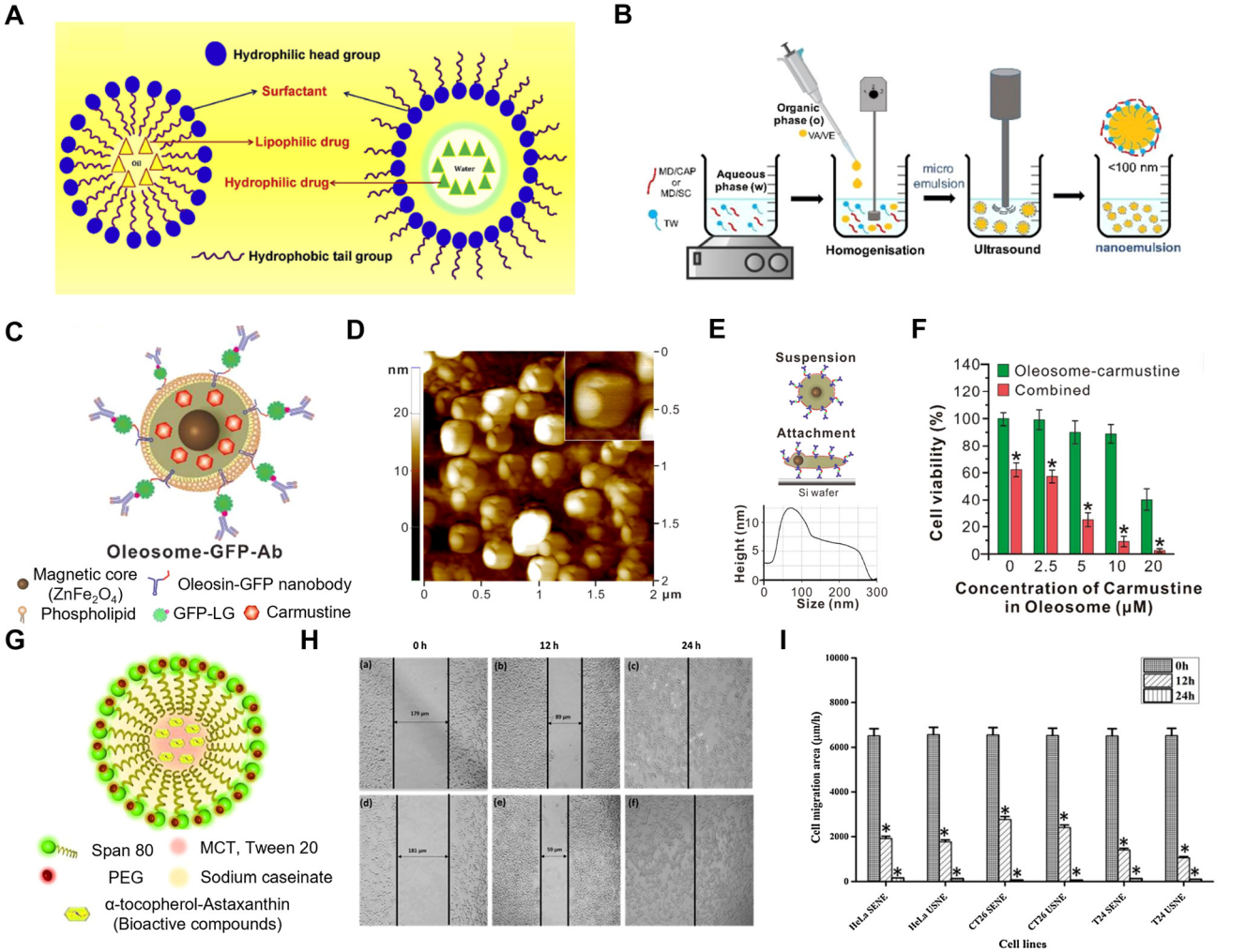

Fig. 5 Structure and synthesis of nanoemulsions. (A) Schematic diagram showing the structure of a nanoemulsion. Reprinted with permission from ref. 56. Copyright 2019, Elsevier. (B) Representative synthesis method for nanoemulsions. Reprinted with permission from ref. 57. Copyright 2019, MDPI. (C) Schematic illustration of a functionalized oleosome, (D) AFM image of an oleosome, (E) measurement of the cross-sectional area was performed along the marked line shown in the inset of (D), and (F) the cytotoxic effects on MDA-MB-231 cells following combined treatment with carmustine and hyperthermia delivered by oleosomes. Reproduced with permission from ref. 58. Copyright 2018, American Chemical Society. (G) Schematic illustration of an ATNE nanoemulsion, (H) *in vitro* wound healing process of ATNE nanoemulsions by scratch assay, and (I) cell migration area in wound healing process of nanoemulsions. Reproduced with permission from ref. 59. Copyright 2018, Elsevier.

physicochemical interactions (*e.g.*, charge) or the unique microenvironmental conditions of the target site. These complementary strategies enable a multifaceted approach to achieving precise and efficient delivery.

Liver-specific ligand-based drug delivery

The liver plays a crucial role in detoxification of the human body. Liver-associated diseases, such as liver fibrosis, viral hepatitis, and hepatocellular carcinoma (HCC), affect approximately 800 million people worldwide, resulting in more than 2 million deaths annually.[62] The mortality of liver-associated diseases has steadily increased over the past 20 years, with chronic liver disease (CLD) and related cirrhosis currently accounting for approximately 1 million deaths annually.[63] Due to limitations in drug treatment, liver resection and transplantation have been assessed as the most successful therapeutic approaches for progressive liver diseases.[64]

The main drawbacks of standard pharmacological therapies for liver treatment include the inability to deliver sufficient drug concentrations to the diseased liver and nonspecific delivery due to systemic circulation. Additionally, drug delivery to specific cells within the liver, such as hepatitis B virus (HBV)-infected cells or hepatic stellate cells (HSC) in liver fibrosis, is required. Therefore, there is a pressing demand for modern chemotherapies that not only enhance the stability of therapeutic agents but also exhibit target specificity for diseased liver cells.[65]

Saccharides. Ligands, such as GalNAc,[66,67] lactose,[68] mannosylated cholesterol derivative cholesten-5-yloxy-*N*-(4-((1-imino-2-β-D-thiomannosylethyl)amino)butyl)formamide (Man-C4-

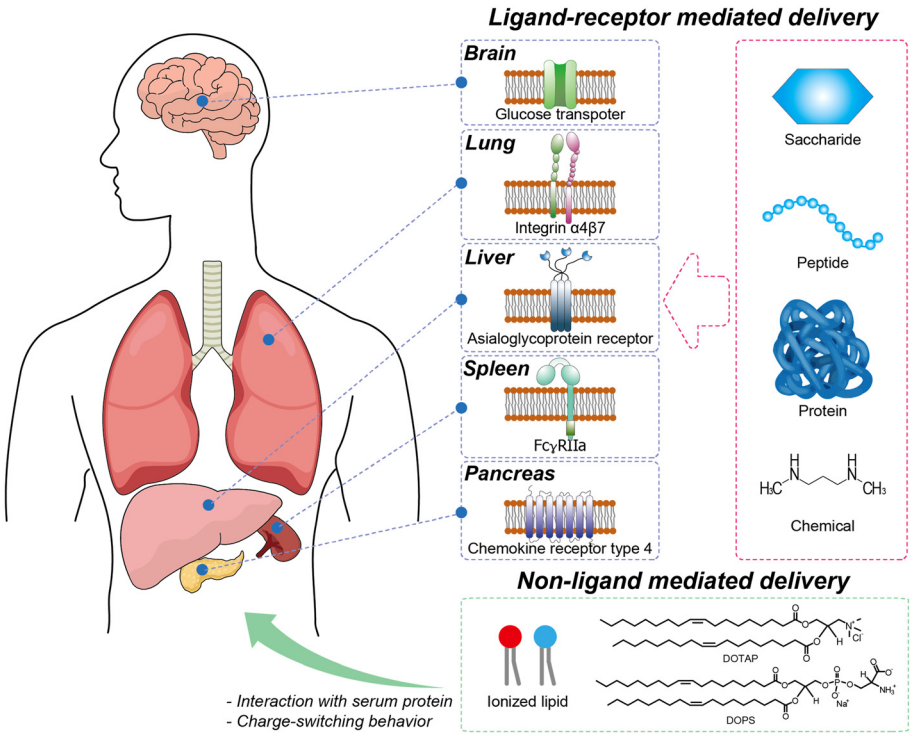

Fig. 6 Methods for organ-specific delivery: ligand–receptor mediated and non-ligand mediated approaches.

Table 1 Summary of targeting ligands for organ-specific delivery

Target organs	Targeting ligands		Particle type	Delivery method	Ref.
	Category	Ligand name			
Liver	Saccharide	GalNAc (*N*-acetyl galactosamine)	LNP	SC/IV	66 and 67
		Lactose	Liposome	IV	68
		Man-C4-Chol	Liposome	IV	69
		Galactose	SLN	IV	70
		Mannan	SLN	IV	71
		DSPE-PEG2000-APM (DPM)	Liposome	IV	72
		DSPE-PEG2000-APF (DPF)			
	Peptide	HBV N-terminal myristoylated preS1/21-47^{myr}-PEG	Liposome	IV	74 and 75
		CKNEKKNKIERNNKLKQPP-peptide	Liposome	IV	76
	Protein	Apolipoprotein A-I	Liposome	IV	77
		Asialofetuin	Liposome	IV	78
		Human serum albumin (HSA) derivatized with *cis*-aconitic anhydride	Liposome	IV	79
Lung	Saccharide	Mannose	LNP	IT	80
	Chemical	D-α-Tocopheryl polyethylene glycol-1000 succinate (TPGS)	Liposome	SC	85
		Nano-calcium phosphate (nano-CaP)	LNP	IV	86
	Peptide	Chol-GALA peptide (WEAALAEALAEALAEHLAEALAEALEALAA)	Liposome	IV	87
		IRQ peptide (IRQRRRR)	Liposome	IV	88
Pancreas	Chemical	PFOB and polymeric CXCR4 antagonists (PCX)	Nanoemulsion	IP	92
		N,*N*-Dimethyl-1,3-propanediamine	Liposome	IV	94
		Thermoresponsive polymer	Liposome	IV	95
		Diethyldithiocarbamate-copper complex $Cu(DDC)_2$ and hyaluronic acid (HA)	Liposome	IV	96
	Peptide	TM4SF5 peptide	Liposome	SC	97
	Protein	Anti-tissue factor (TF) antibody	Liposome	IV	98
Brain	Saccharide	Glucose	Liposome	IV	109
	Peptide	RGD peptide	Liposome	IV	110
		AP-1 peptide	Liposome	IV	111
		RGD tripeptide and lactoferrin	Liposome	IV	112
	Protein	TPGS-Tf	Liposome	IV	116
		8D3 antibody	Liposome	IV	117
	Others	Cell membrane fragment (CMF)	Liposome	SC	118

CholI),[69] galactose,[70] mannan,[71] and 4-aminophenyl-α-D-mannopyranoside (APM)/4-aminophenyl-β-L-fucopyranoside (APF),[72] can be used to achieve specific delivery to the liver. Among these, GalNAc stands out due to its strong affinity for the asialoglycoprotein receptor (ASGPR), a liver-specific receptor predominantly expressed on hepatocytes. ASGPR plays a pivotal role in receptor-mediated drug delivery by facilitating cellular internalization through clathrin-mediated endocytosis. Its high specificity for hepatocytes and minimal expression in extrahepatic cells make it an attractive target for achieving precise liver targeting with reduced off-target toxicity.[66,73] Through the recognition of exposed galactose by ASGPR, GalNAc-PEG-LNP (prepared by conjugating GalNAc to LNPs with PEGylation) achieves liver targeting through the process of endocytosis. The GalNAc-LNPs, with particle sizes ranging from 50 to 70 nm, were administered through IV injection. Approximately 90% of the injected LNPs accumulated in the liver, while the remaining were accumulated in the spleen (Fig. 7A–C).

Additionally, APM and APF have been used to interact with the mannose/fucose receptors highly expressed in Kupffer cells (KCs).[72] For the synthesis of the dual-ligand modified PEGylated liposomes (MFPLs), APM and APF were mixed with the PEGylated derivative of phospholipid 1,2-distearoyl-*sn*-*glycero*-3-phosphorylethanolamine (DSPE) DSPE-PEG2000-NHS. The resulting DSPE-PEG2000-APM (DPM) and DSPE-PEG2000-APF (DPF) were mixed with liposomes to finally synthesize MFPLs with a size of 180–200 nm (Fig. 7D). Flow cytometry analysis of KCs treated with nicotinamide riboside (NR) liposomes for 4 h at 37 °C revealed that the MFPL5-5 group (with an HSPC : CH : DPM : DPF ratio of 3.0 : 1.0 : 0.5 : 0.5), exhibited the highest targeting efficiency among all the formulations (Fig. 7E). Following their IV injection into rats, the synthesized MFPLs demonstrated significantly superior liver targeting compared to a control without ligands (Fig. 7F).

Peptides. Another approach for targeting the liver involves using peptides, such as myristoylated preS1/21-47 (preS1/21-47^{myr})[74,75] and CKNEKKNKUERNNKLKQPP,[76] as ligands. The preS1/21-47^{myr} peptide mimics the surface protein of HBV and targets the scavenger receptor class B type 1 (SR-B1), promoting the cellular uptake of drugs.[74] The preS1/21-47^{myr} peptide, synthesized through PEGylation of liposomes and maleimide–thiol coupling reaction, is approximately 120 nm in size. When administered by IV, pre-S1/21-47^{myr} liposomes demonstrated enhanced targeted delivery to the liver compared to the control group without preS1/21-47^{myr}, indicating significantly improved liver targeting.

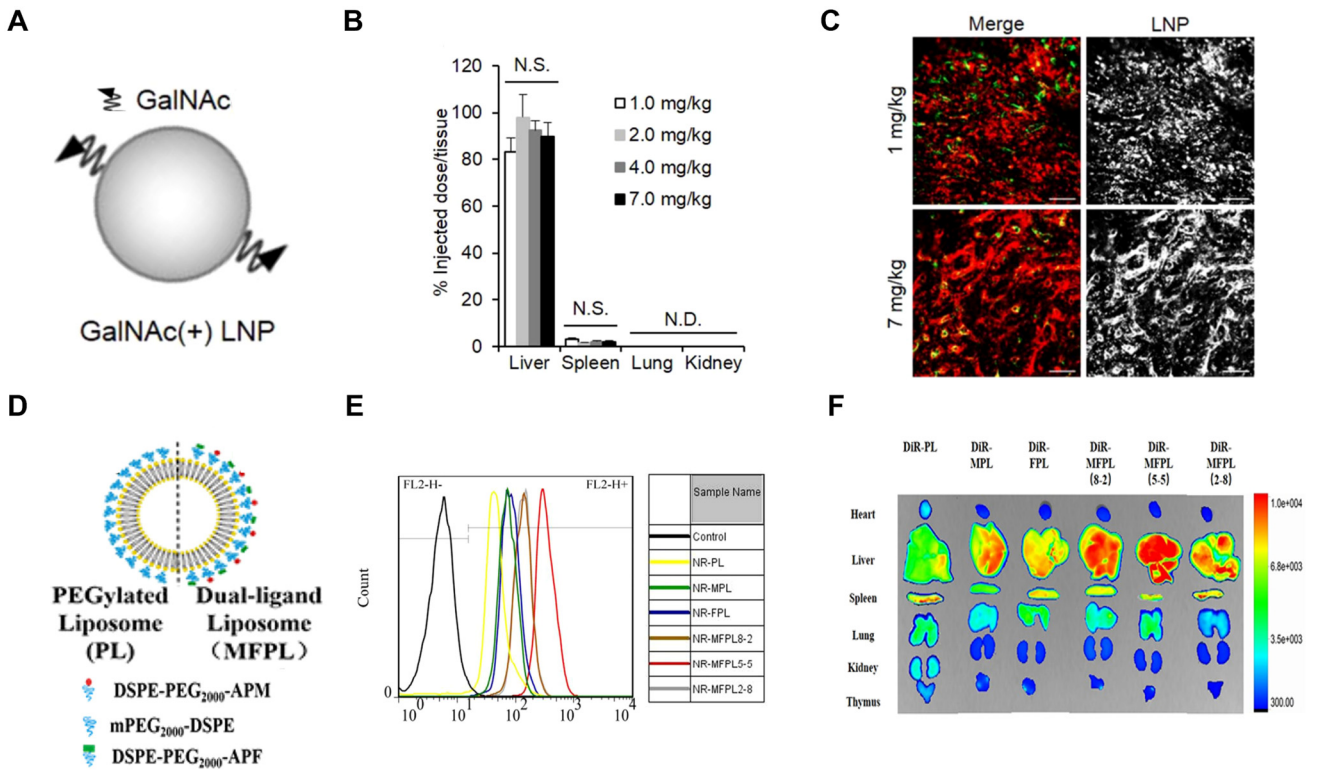

Fig. 7 Particle functionalization using ligands for targeting the liver. (A) LNP modified by GalNAc for liver-specific delivery, (B) the efficiency of GalNAc(+) LNPs. IV injection of GalNac(+) LNPs delivers particles specifically to the liver, and (C) tissue distribution of the LNPs was determined 30 min after LNP injection. Reproduced with permission from ref. 66. Copyright 2017, Elsevier. (D) Liposome functionalized by a dual-ligand, (E) cytometry analysis of KCs treated with NR liposomes, and (F) the biodistribution of dual-ligand liposomes in multiple organs. Compared to the control, IV-injected dual-ligand liposome shows greater liver specificity. Reproduced with permission from ref. 72. Copyright 2018, American Chemical Society.

Proteins. Similarly, proteins, such as apolipoprotein A-I (apoA-I),[77] asialofetuin,[78] and human serum albumin, can be used as ligands for targeting the liver.[79] Using apoA-I as a ligand, high-density lipoprotein (HDL) employs a mechanism that takes advantage of its hydrophobic cholesterol ester-loading properties to serve as a carrier for delivering lipophilic antitumor drugs to human HCC cells.[77] ApoA-I, which is a protein component of HDL, guides the transportation of cholesterol from arterial wall cells to the liver and steroid-producing organs. ApoA-I can be employed to deliver drugs to the liver through cell-surface receptors, such as SR-BI (for mice) or cytosolic iron–sulfur protein assembly (CIA-1; for humans). Moreover, as apoA-I is an endogenous product of the liver, its use as a ligand in HDL-based drug delivery systems does not induce immunological side effects during clinical applications.

To synthesize particles that can be selectively delivered to the liver, apoA-I was combined with nucleic acid-loaded cationic liposomes and suspended overnight in a 5% dextrose solution at 4 °C. The synthesized apoA-I–liposomes were approximately 180 nm in size. In a mouse model with HBV replication, the administration of 2 mg kg^{-1} of DTC-Apo/siHBV nanoparticles resulted in a significant RNA interference effect, with reductions in serum HBV surface antigen expression by 65.1% on day 2, 63.4% on day 4, 74.9% on day 6, and 72.8% on day 8. These findings suggest that siRNA-based therapies utilizing apoA-I as a ligand represent a promising approach for treating viral hepatitis such as HBV.

Lung-specific ligand-based drug delivery

Acute and chronic lung diseases have some of the highest mortality rates, and obstructive lung diseases are considered one of the top four leading causes of death worldwide.[80] Furthermore, the lungs have relatively low levels of drug-metabolizing enzymes compared to other organs, such as the liver, pancreas, and spleen, leading to lower drug efficacy. Therefore, there is a need to maximize the efficiency of drug delivery to the lungs by increasing the amount of drug delivered through specific targeting to the lungs.[81] Over the years, researchers have developed lung-specific ligand systems, such as chemical ligands, peptides, proteins, and ionized lipids, to enhance both the delivery efficiency and specificity of drug-loaded nanoparticles.[82] For example, the α4β7 integrin has demonstrated a superior ability to interact with vascular cell adhesion molecule-1 (VCAM-1), a molecule expressed by lung-specific epithelial cells. This interaction facilitates precise targeting and efficient delivery of therapeutic agents to the lungs.[83]

Saccharides. Mannose-functionalized LNPs have been developed for the treatment of pulmonary fibrosis.[84] In this study, PEG lipids containing a mannose ligand were incorporated into the LNPs to target the CD206 receptor, which is overexpressed during inflammatory processes. This design enabled the mannose-LNPs to effectively deliver siRNA targeting G2 and S phase-expressed protein 1 (GTSE1), a fibrosis-related protein, to epithelial, endothelial, and immune cells in a pulmonary fibrosis animal model, resulting in approximately a 50% reduction in collagen accumulation. As a result, the epithelial–mesenchymal transition (EMT) process was inhibited, fibrosis-related protein expression decreased, and lung function showed significant improvement.

Chemicals. D-α-Tocopheryl polyethylene glycol-1000 succinate (TPGS) and nano-calcium phosphate (nano-CaP) are representative chemical agents used for targeted drug delivery to the lungs.[83,85] Therapeutic agents loaded into TPGS-liposomes have demonstrated specific delivery in the lungs through subcutaneous (SC) injection. TPGS is a non-ionic surfactant that inhibits P-glycoprotein (P-gp), a cause of multidrug resistance (MDR), and can avoid recognition by the reticuloendothelial system, leading to prolonged systemic circulation. Following SC injection of TPGS-coated DTX-loaded liposomes into mice with lung tumors, a tumor inhibition efficiency of approximately 74.6% was achieved, which was significantly increased compared to that of the control group.

Exploiting the pH-sensitivity of CaP, Sethuraman *et al.* developed LNPs loaded with lumefantrine (LF) and nano-CaP (so-called LF-CaP-Ls) (Fig. 8A) for enhanced lung-targeted delivery efficacy in treating lung cancer (Fig. 8B).[86] Pulmonary histopathology evaluation was conducted following the administration of LF-CaP-Ls *in vivo* (Fig. 8C). The results revealed reduced tumor vasculature in blood vessels and inflammatory cells, as well as a reduced rate of lung cancer progression in the LF-CaP-Ls treatment groups compared to those treated with LF, Ls, and LF-Ls. Additionally, no organ bleeding was noted.

Peptides. To deliver drug-loaded nanoparticles to the lungs unaffected by the bloodstream, peptides are commonly used to create ligands with enhanced stability and targeted delivery efficiency. The GALA (WEAALAEALAEALAEHLAEALAEALEALAA) and IRQ (IRQRRRR) peptides are representative ligands used in nanoparticles for lung-targeted delivery of therapeutics (Fig. 8D and E).[87,88] The GALA peptide is an endosomal destabilizer inspired by viral mechanisms. During experiments, liposomes containing the GALA peptide also exhibited the functionality of the IRQ peptide in targeting the lung endothelium. GALA peptide-liposomes recognize and bind to integrin $\alpha_4\beta_7$ on the surface of human lung microvascular endothelial cells (HMVEC-Ls) with superior uptake in HMVEC-Ls and human umbilical vein endothelial cells (HUVECs) compared to HepG2, A549, and HeLa cells, suggesting that more accurate lung-specific target delivery is possible (Fig. 8F). In addition, the GALA peptide-liposomes recognize and bind to the sialic acid-terminated sugar chains on the surface of HMVEC-Ls. Upon IV administration, GALA peptide-liposomes began to show lung accumulation within 5 min. After 6 h, their accumulation in lung tissue was 24 times higher compared to liposomes without the GALA peptide, highlighting the effectiveness of the GALA peptide in achieving lung-specific delivery and drug efficacy.

Pancreas-specific ligand-based drug delivery

Because of the pancreas' anatomical location (intra-abdominal region) and intricate composition, the process of detecting

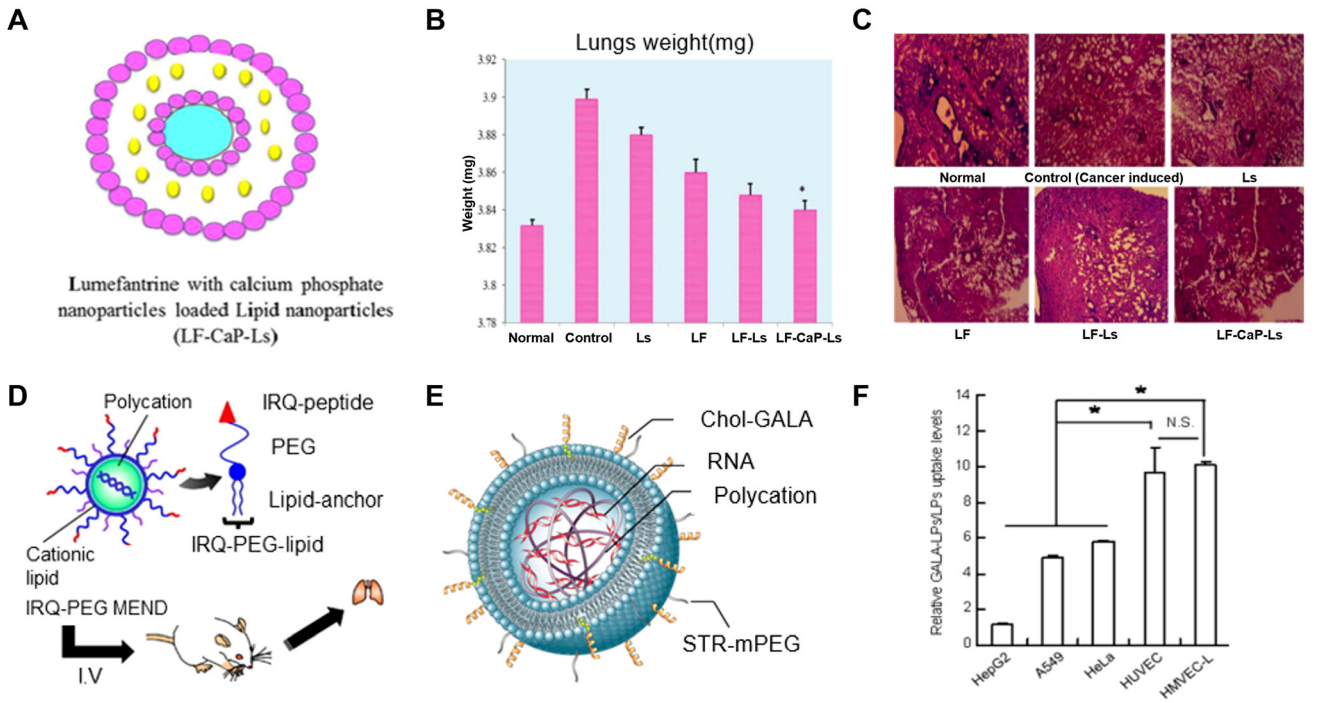

Fig. 8 Particle functionalization using ligands for targeting the lung. (A) Nano-CaP-loaded LNPs (LF-CaP-Ls), (B) graphical representation of the lung weights in different treatment groups, and (C) histopathology examination of lungs from different treatment groups (normal, control, and tumor-bearing mice treated with LF, LF-Ls, LF-CaP-Ls) using H&E staining and viewed under a light microscope at ×10 magnification. Reproduced with permission from ref. 86. Copyright 2021, Elsevier. (D) Liposome composed of PEG-lipid modified with IRQ peptide delivery to the lungs by IV injection into the rat tail. Reproduced with permission from ref. 88. Copyright 2011, Elsevier. (E) Schematic diagram of GALA peptide-modified liposome particle for lung-specific delivery, and (F) relative cellular uptake of GALA-LPs to LPs by nonendothelial cells (HepG2, A549, and HeLa) and endothelial cells (HMVEC and HUVEC). Reproduced with permission from ref. 87. Copyright 2013, American Chemical Society.

and localizing pancreatic diseases presents significant challenges, which can result in delays in the implementation of suitable therapy and management strategies for disorders that affect this organ.[89] In addition, there is also a lack of well-established medical therapies for many pancreatic diseases, including pancreatitis, pancreatic cancer, and other pancreatic disorders. Due to the inherent difficulties associated with treating pancreatic diseases, the focus has been mainly placed on palliative care as opposed to curative interventions. The use of nanoparticles for drug delivery, with a particular focus on targeting the pancreas, has significant potential to revolutionize this prevailing paradigm.[90,91] Nanoparticle-based therapy presents a promising opportunity to provide treatment at reduced dosages while concurrently attaining desired therapeutic effects, which are both targeted and particular.

Chemicals. When using ligands as chemicals for pancreatic targeting, it is important to consider high pancreatic penetration efficacy. Therefore, in the synthesis of nanoemulsions, perfluorooctylbromide (PFOB) and polymeric C–X–C chemokine receptor type 4 (CXCR4) antagonists (PCX) have been used as they support pancreatic penetration efficacy and provide stability to the nanoemulsion structure (Fig. 9A).[92] CXCR4 is a receptor for stromal cell-derived factor-1 (SDF-1). By exploiting this interaction, SDF-1-coated particles enable specific delivery to $CXCR4^{+}$ pancreatic cancer cells.[93] The addition of PCX allows the nanoemulsion to specifically target and bind to CXCR4, which is strongly expressed in pancreatic cancer, allowing the encapsulated drug to diffuse into pancreatic cancer cells. When administered IP, the prepared nanoemulsion shows a more targeted and effective approach to treating pancreatic cancer compared to IV injection (Fig. 9B and C).

N,*N*,*N*′-Trimethyl-*N*′-(2-hydroxy-3-methyl-5-[^{123}I]iodobenzyl)-1,3-propanediamine, abbreviated ^{123}I-labeled HMPDM, is used as a pancreatic contrast agent and is highly effective for specific pancreatic delivery, possessing a strong capability to penetrate the blood–pancreas barrier. Additionally, *N*,*N*-dimethyl-1,3-propanediamine (DMPA) is a ligand that enables the targeting of 1,2-distearoyl-*sn*-glycero-3-(L-1,2-distearin) (DSCP) to the pancreas.[94] Liposomes created using these two chemicals can be IV injected and exhibit remarkable improvements in pancreatic cell-specific delivery efficiency compared to the control. Their delivery efficiencies exceeded 1.7- and 2.1-fold, respectively. Furthermore, the therapeutic effect of the drug delivered by these liposomes demonstrated excellent signal detection.

Moreover, particles coated with a thermoresponsive polymer on their surface have shown the ability to induce specific delivery to the pancreas when administered by IV. In addition, liposomes have been engineered to specifically target the pancreatic stem cancer stem cell marker CD44 receptor by encapsulating diethyldithiocarbamate-copper $Cu(DDC)_2$ in

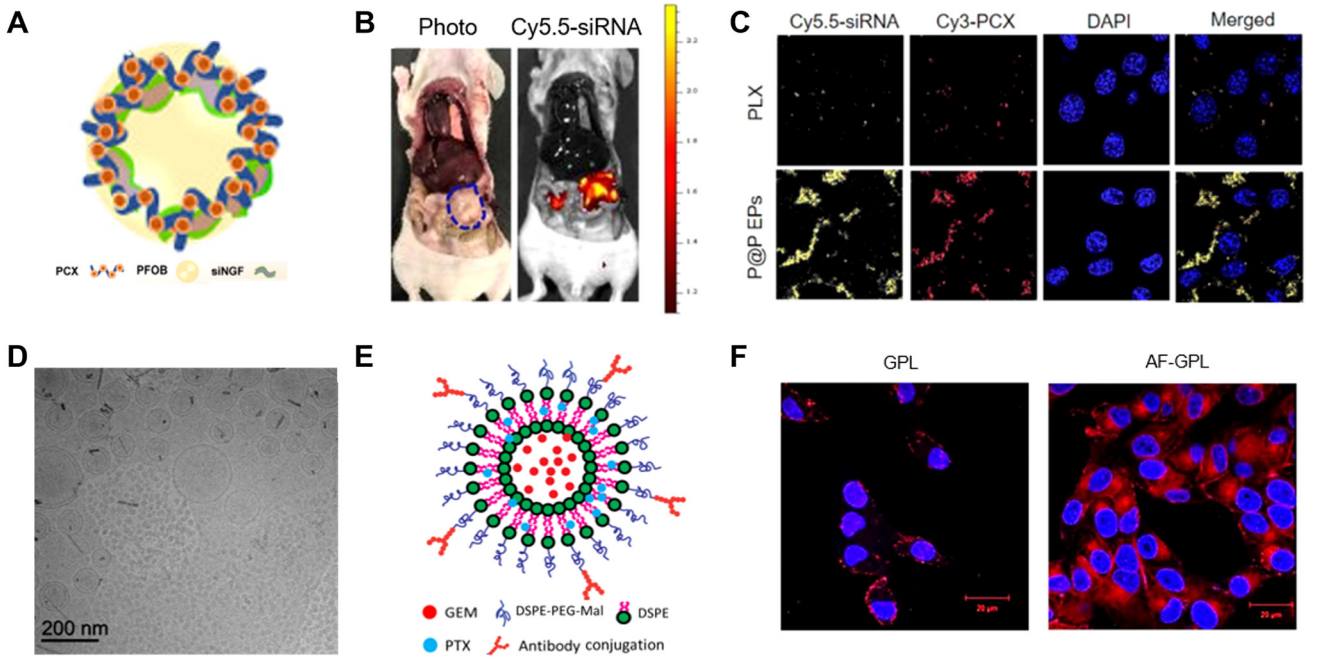

Fig. 9 Particle functionalization using ligands targeting the pancreas. (A) Nanoemulsion modified with PFOB and PCX for pancreatic cancer treatment, (B) fluorescence image captured 24 h after injection of particles loaded with Cy5-mLuc to show pancreatic target delivery, and (C) confocal microscopy observation of the KPC8060 cells after treatment with P@P EPs or PLX. Reproduced with permission from ref. 92. Copyright 2022, American Chemical Society. (D) $Cu(DDC)_2$-loaded liposomes. Reproduced with permission from ref. 96. Copyright 2019, Elsevier. (E) Schematic presentation of a preparation of gemcitabine and paclitaxel-loaded liposomes conjugated with AF, and (F) confocal laser scanning microscopy confirming the binding efficiency of GPL and AF-GPL for pancreatic cancer cells. Reproduced with permission from ref. 98. Copyright 2018, Elsevier.

HA-decorated liposomes (Fig. 9D).[95,96] HA is the principal ligand of the CD44 receptor, which exhibits heightened expression levels in pancreatic cancer cells as well as other pancreatic diseases. Following IV injection, the $Cu(DDC)_2$-loaded HA-decorated liposomes exhibited targeted affinity toward the pancreas, thereby improving the accuracy of drug delivery and potentially augmenting the effectiveness of therapy.

Peptides. Using peptides that can specifically bind to substances that are overexpressed in a diseased pancreas offers a promising approach to the synthesis of particles capable of precise and specific pancreatic delivery. Previous studies have confirmed overexpression of tetraspanin transmembrane 4 superfamily member 5 (TM4SF5) in pancreatic cancer tissues, making it an attractive target for specific therapeutic interventions. By leveraging this knowledge, researchers can create suitable nanoparticles for targeting pancreatic cancer cells.[97] To achieve pancreas-targeted delivery, TM4SF5 peptide epitope-CpG-DNA-liposome complexes can be prepared such that the liposomes are coated with the TM4SF5 peptide or TM4SF5 cDNA. Moreover, these TM4SF5-targeted nanoparticles can be administered by SC injection, providing a minimally invasive route for drug delivery. Administration of this complex vaccine to mice showed high specific delivery efficiency to the pancreas and tumor growth inhibition compared to the control group. The tumor weight also showed a reduction of up to 2 g, indicating that the developed liposome complex enhanced the effect of the vaccine.

Proteins. The advantage of using antibodies as smart ligands for nanoparticle-based drug delivery systems in cancer treatment is their high affinity and specificity. Anti-tissue factor (TF) is overexpressed on the surface of pancreatic cancer cells and other cancer cells, and the TF antibody fragment (AF) is a peptide that specifically binds to TF. By conjugating TF AF to the surface of liposomes, these liposomes can effectively recognize and bind to TF on the surface of cancer cells (Fig. 9E). This tumor-targeting approach allows for the preferential delivery of liposomes containing the therapeutic drug to cancer cells, such as those present in pancreatic tumors, thereby enhancing the therapeutic effect and reducing off-target effects on healthy tissues.[98] AF-conjugated liposomes have shown enhanced cellular uptake in pancreatic cancer cells compared to non-targeted liposomes (Fig. 9F). Furthermore, the drug delivered through AF-conjugated liposomes exhibited significantly higher cytotoxic effects in pancreatic cancer cells compared to non-targeted drug delivery.

Brain-specific ligand-based drug delivery

Alzheimer's disease,[99–101] Parkinson's disease,[102–104] and brain tumors[105] have become major health issues worldwide, with high mortality and morbidity rates, imposing a significant burden on societies. However, current treatments mostly alleviate symptoms of brain diseases without achieving satisfactory therapeutic effects at the fundamental level.[106] Extensive research suggests that the efficacy of brain disease treatments

is primarily influenced by two factors: the preservation of the BBB and the complexity of the brain's microenvironment.[107] In an attempt to overcome these factors and facilitate delivery to the brain, a method involving the exposure of ligands on the surface of nanoparticles is being explored for targeted and specific nanoparticle delivery. Therefore, in this section, we introduce methods to overcome the challenge imposed by the BBB in reaching the brain.

Saccharides. In the brain, glucose transporters (GLUT1-6 and GLUT8) and Na^+-D-glucose cotransporters (SGLT1) play a critical role in facilitating glucose diffusion. These transporters mediate the uptake of D-glucose across the blood–brain barrier (BBB), offering a potential pathway for drug delivery systems utilizing D-glucose as a transport mechanism to the brain.[108] By displaying glucose on the surface of liposomes, targeted delivery through the glucose transporters at the BBB can be achieved. To address the bidirectional transport limitation of the BBB GLUT1, a thiamine disulfide system (TDS) with a "lock-in" capability was conjugated to glucose and subsequently linked to cholesterol.[109] This glucose-modified liposome (L-TDS-G) was then employed to deliver docetaxel (DTX). The results demonstrated that this approach was approximately 56.6% more efficient than using naked DTX, highlighting the effectiveness of the glucose-modified liposome for brain-targeted drug delivery.

Peptides. Peptides have been used as ligands as an alternative approach to facilitate drug delivery to the brain. Particles have been improved by decorating their surfaces with RGD peptides, activator protein 1 (AP-1) peptides, and other variants.[110–112] When RGD peptide was attached to the surface of liposomes (Fig. 10A), it enabled passage through the cerebral microvascular endothelial cells of the BBB *via* the integ-

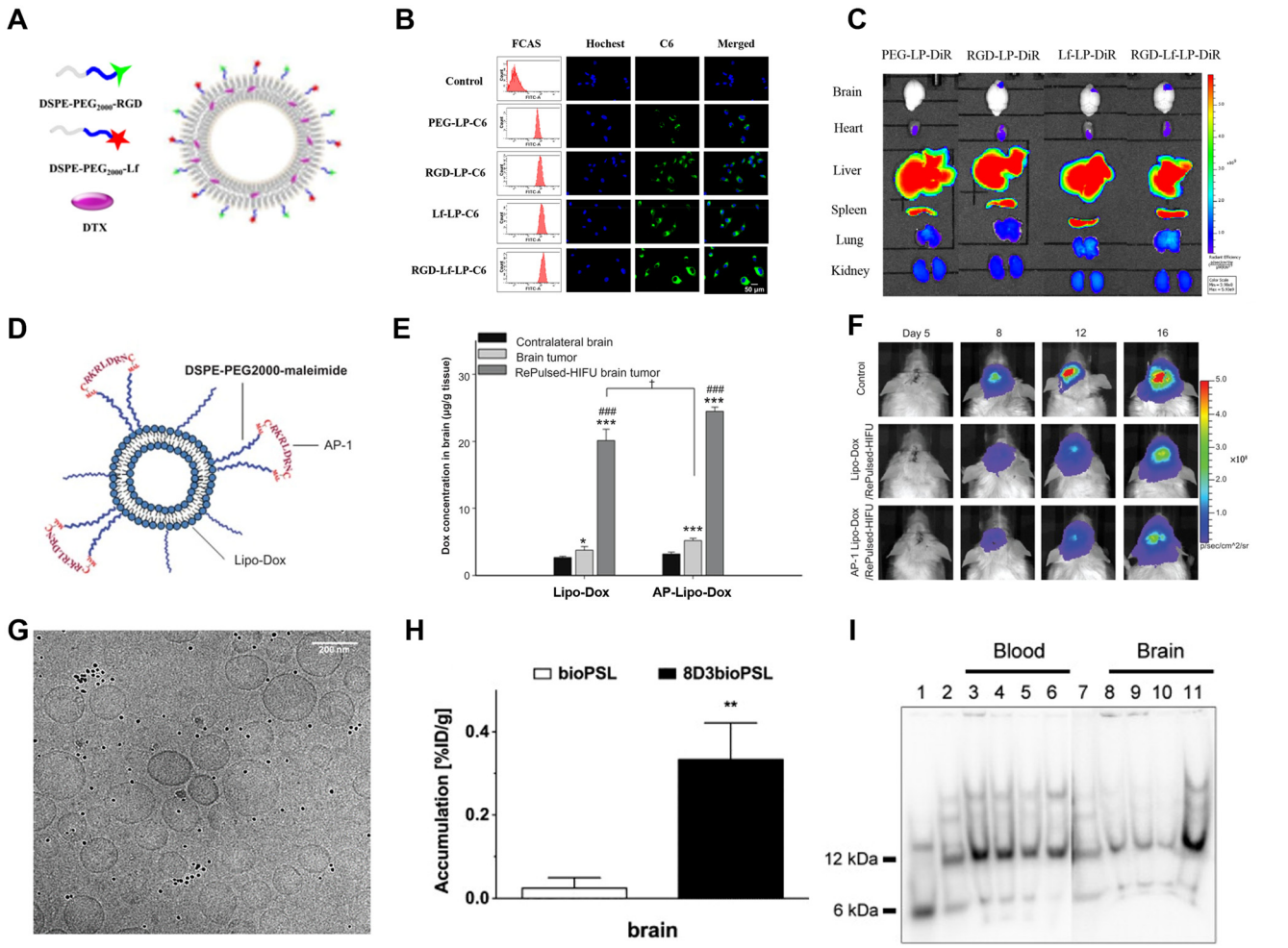

Fig. 10 Particle functionalization using ligands for targeting the brain. (A) Schematic illustration of brain-targeted liposomes functionalized by RGD peptide and luciferin, (B) fluorescence microscopy images of cellular uptake *in vitro*, and (C) biodistribution of liposomes shows increased brain delivery when ligands are conjugated. Reproduced with permission from ref. 112. Copyright 2021, Springer Nature. (D) Schematic illustration of brain-targeted liposomes functionalized by AD-1 peptide, (E) comparison of the doxorubicin concentration in the brain between liposomes and ligand-conjugated liposomes, and (F) bioluminescence image of a brain tumor shows a decrease in tumor size following administration of liposomes with conjugated ligands. Reprinted with permission from ref. 111. Copyright 2012, Dove Medical Press Ltd. (G) Cryo-TEM image of a brain-targeted liposome functionalized by antibody 8D3, (H) brain accumulation of bioPSL and 8D3bioPSL, and (I) analysis of ODN integrity in the blood or brain by PAGE. Reproduced with permission from ref. 117. Copyright 2008, Elsevier.

rin $\alpha_v\beta_3$ receptor, thereby promoting delivery to brain tumors,[113,114] and the addition of the glycoprotein lactoferrin further enhanced BBB penetration through the lactoferrin receptor; both ligands were conjugated to the liposome's constituent lipids using PEG, and these ligand-conjugated liposomes increased the cellular uptake *in vitro* (Fig. 10B). *In vivo* imaging of the orthotopic glioma taken from U87 MG orthotopic tumor-bearing nude mice given a tail vein injection of the RGD-modified DTX-loaded liposomes containing DiR dye showed a 1.29-fold increase in the cerebral fluorescent signal compared to that of the PEG-liposome, and a relative increase of 3.35-fold was observed when RGD and lactoferrin dual-modified liposomes were injected (Fig. 10C).[112] Furthermore, by binding maleimide to DSPE, a liposome component, liposomes were functionalized through coupling with the AP-1 peptide through a thiol-maleimide reaction (Fig. 10D). *In vivo* experiments conducted *via* IV injection confirmed that the AP-1 peptide-conjugated liposomes exhibited increased delivery efficiency of doxorubicin to the brain compared to conventional liposomes (Fig. 10E), and a reduction in brain tumor size was observed through bioluminescence imaging (Fig. 10F).

Additionally, RVG29 peptide-functionalized SLNs have been developed as a drug delivery system targeting Alzheimer's disease.[115] The RVG29 peptide selectively binds to nicotinic acetylcholine receptors (nAchRs) expressed on neurons and the BBB, thereby enhancing drug delivery efficiency across the BBB. This system was designed to encapsulate quercetin, a neuroprotective compound known for its antioxidant and anti-inflammatory properties, effectively inhibiting amyloid-beta (Aβ) aggregation associated with AD. The study demonstrated that RVG29-functionalized SLNs exhibited a 1.5-fold increase in BBB permeability compared to non-functionalized nanoparticles and successfully inhibited Aβ aggregation. These findings showed promise for the use of RVG29-SLN as a drug delivery system and neuroprotective strategy for the treatment of Alzheimer's disease in an *in vivo* model.

Proteins. The glycoprotein transferrin (Tf) was modified by introducing carboxyl groups using succinic anhydride and then coupled with TPGS through *N*-(3-dimethylaminopropyl)-*N*′-ethylcarbodiimide (EDC)/*N*-hydroxysuccinimide (NHS) coupling to form TPGS-Tf. TPGS-Tf enables brain delivery by interacting with Tf receptors present in the BBB.[116] TPGS-Tf exhibited approximately 4.41- to 8.91-fold greater delivery efficiency compared to non-functionalized liposomes. Additionally, liposomes were conjugated with 8D3, a rat antibody that binds to transferrin receptor 1, TfR1 (Fig. 10G).[117] When 8D3 antibody-conjugated liposomes were delivered to a mouse model *via* IV injection, brain-targeted efficacy was increased compared to conventional liposomes (Fig. 10H). Subsequently, polyacrylamide gel electrophoresis (PAGE) analysis, performed to determine intact octadecaneuropeptide (ODN) in the brain at each time point, confirmed that the ^{32}P signal was similar to the radioactivity counting shown in pharmacokinetic studies (Fig. 10I).

Others. Another approach involved using natural killer (NK) cell membrane fragments (CMF) as ligands for specific brain delivery.[118] Major histocompatibility complex (MHC) class I polypeptide-related sequence A and B (MICA/B) and the member of retinoic acid early transcripts-1 (RAET1H), both of which are ligands of natural killer group 2 member D (NKG2D), are upregulated on the surfaces on cells under oxidative stress and they have a high affinity with NKG2D expressed on NK cell membranes. With this in mind, curcumin-loaded NK cell membrane biomimetic nanocomplexes were prepared for brain-targeted therapy through the meningeal lymphatic vessels (MLV) route. Nanoparticles coated with CMF exhibited an intracellular delivery efficiency of more than 2-fold greater than that of conventional nanoparticles, while the BBB permeability was also found to increase by approximately 20-fold.

Non-ligand functionalized LBNs for organ-specific delivery

Ionized lipids play a critical role in organ-targeted delivery by enabling specific interactions with organ-specific cells or extracellular environments, improving biodistribution, and enhancing therapeutic efficacy. Through their unique charge-switching behavior, ionized lipids remain neutral at physiological pH but become protonated under acidic conditions (*e.g.*, within endosomes or tumor microenvironments), facilitating enhanced cellular uptake and endosomal escape. In the context of organ-targeted delivery, ionized lipids are frequently incorporated into LNPs to enable selective accumulation in target tissues through active targeting strategies or passive mechanisms.[119] This section explores how ionized lipids are utilized for organ-specific delivery to the liver, lungs, pancreas, and spleen (Table 2).

Liver-targeted ionized lipids. Ionized lipids, such as cationic selective organ-targeting (SORT) lipids,[120] can be employed as liver-targeting ligands. It is thought that after IV administration, nanosized particles are surrounded by a plasma protein corona upon their interaction with biological fluids, which can alter the surface properties of nanoparticles and determine their *in vivo* fate. While the composition of this corona is affected by factors such as the physical properties of the nanoparticles and the physiological conditions, the protein corona surrounding LNPs is typically rich in apolipoprotein E (apoE). The interaction between LNPs and the N-terminal lipid-binding region of apoE causes conformational changes in apoE, which results in a high affinity to hepatic low-density lipoprotein receptors (LDL-Rs), thereby facilitating hepatocyte cell entry.[121] The ionized lipid-based SORT LNPs allow for different target organs depending on the charge of the lipids. SORT LNPs are designed to selectively work target cell types, including epithelial cells, endothelial cells, B cells, T cells, and hepatocytes.[120] For liver hepatocyte-targeting, 1,2-dioleoyl-3-dimethylammonium propane (DODAP) cationic SORT lipids with tertiary amino groups were mixed at a ratio of 20% with traditional LNPs. As a result, DODAP LNPs showed a 20% efficiency of target-specific delivery to the liver when administered through IV injection in mice.

LNP delivery platforms have been developed for gene editing therapeutics. LNPs formulated with lipids containing ester 306-O12B (O-series) bonds in their tails were shown to

Table 2 Summary of ionized lipid for organ-specific delivery

Target organs	Ionized lipid name	Particle type	Delivery method	Ref.
Liver	Cationic selective organ-targeting (SORT) lipids (DODAP)	LNP	IV	120
	306-O12B lipid	LNP	IV	122
Lung	Cationic SORT lipids (1,2-dioleoyl-3-trimethylammonium propane, DOTAP)	LNP	IV	120
	DOTAP	Liposome	IP	123
	1,2-Dipalmitoyl-*sn-glycero*-3-phosphocholine (DPPC)			
	306-N16B	LNP	IV	124
Pancreas	Cationic helper lipid ($306O_{i10}$, $514O_{6,10}$)	LNP	IP/IV	125
Spleen	1,2-Dioleoyl-*sn-glycero*-3-phospho-L-serin (DOPS)	Liposome	IV	128
	OF-Deg-Lin	LNP	IV	129
	Anionic SORT lipids (18PA)	LNP	IV	120

deliver Cas9 mRNA and angiopoietin-like 3 (Angptl3)-specific single-guide RNA (sgRNA) (sgAngptl3) efficiently to the hepatocytes for knockdown of the *angptl3* gene, which is a promising therapeutic target for the treatment of human lipoprotein metabolism disorders.[122] The optimal formulation for the LNPs was determined to be 50% 306-O12B, 38.5% cholesterol, 10% 1,2-dioleoyl-*sn-glycero*-3-phosphocholine (DOPC), and 1.5% 1,2-dimyristoyl-*rac-glycero*-3-methoxy PEG2000 (DMG-PEG) (molar basis), with a 7.5 : 1 weight ratio of 306-O12B to mRNA. Firefly luciferase mRNA (fLuc mRNA)-encapsulated 306-O12B LNPs had an average diameter of 112 nm. The fLuc mRNA LNPs formulated with DOPC resulted in significantly higher luciferase expression in the livers of Ai14 reporter mice compared to that observed when the mice were treated with formulations containing 1,2-dioleoyl-*sn-glycero*-3-phosphoethanolamine (DOPE) and the original distearoyl phosphatidylcholine (DSPC) phospholipid. Then, wild-type C57BL/6 mice were injected with 306-O12B LNP coformulated with different Cas9 mRNA-to-sgAngptl3 mass ratios of 2 : 1, 1 : 1.2, and 1 : 2 at a total RNA dose of 3.0 mg kg^{-1}. Although the ratio was expected to affect the *in vivo* genome editing efficacy, the results showed no significant differences among the groups. It appears that the detailed ligand–receptor mechanism has not been elucidated, indicating the need for further research.

Lung targeted ionized lipids. Researchers have investigated several modified ionized lipids for targeted delivery of drugs to the lungs. The most effective agents for lung-specific delivery among the examined SORT and N-series lipids (contain amide bonds in their tails) are two unique modified ionized lipids: dioleoyl trimethylammonium propane (DOTAP) and 306-N16B. Two key components used in the synthesis of liposomes are the cationic lipid, DOTAP, and the major pulmonary surfactant, DPPC. It should be noted that the 306-N16B LNPs have different organ tropism from 306-O12B LNPs, which is thought to be due largely to the differences in the protein compositions, fractions, and biological functions of the coronas between these two LNPs. Among the proteins in the corona of DOTAP, vitronectin (Vtn) exhibits the most affinity for DOTAP. Vtn recognizes $\alpha_5\beta_3$ integrin, which is expressed primarily in the epithelial cells of the lung.[121] By encapsulating unmethylated cytosine–guanine dinucleotide (CpG) motifs within these liposomes, they can be effectively targeted to the lungs through intraperitoneal (IP) injection. CpG motifs are powerful immunostimulatory agents recognized by toll-like receptors (TLRs) present in certain immune cells, including pulmonary macrophages.[120] The loading of CpG motifs into cationic liposomes and their administration through injection in a mouse model of lung cancer demonstrated remarkable potential for achieving localized delivery to the lungs and eliciting an anti-tumor immune response.[123] By specifically targeting pulmonary macrophages through IP injection, the CpG-loaded cationic liposomes effectively delivered the immunostimulatory CpG motifs to the lungs. Compared to the control group, a reduction in tumor cell count of approximately 6-fold was observed, and the capture of the liposomes in the lungs was permanent, leading to a favorable prognosis.

The incorporation of 306-N16B with DOPC has proven to be highly effective in inducing the highest fluorescence protein expression efficiency in the lungs. LNPs modified with 306-N16B can efficiently adsorb onto unique plasma proteins present on the lung surface upon IV injection.[124] This led to a transfection efficiency of 33.6%, resulting in excellent lung-specific delivery and significantly improved expression efficiency.

Pancreas targeted ionized lipids. Another approach to minimize the off-target delivery of LNPs designed for IP injection and enable specific delivery to the pancreas is by modifying the charge of the helper ionized lipid. Several experimental studies have demonstrated that the inclusion of both cationic and anionic helper lipids in LNP formulations is crucial for achieving effective pancreatic-specific targeting. While cationic lipids alone may contribute to improved targeting to some extent, they are insufficient to achieve optimal results. The addition of ionizable lipids to the LNP formulation is essential to enable specific delivery and expression in the pancreas. LNPs that contain the anionic lipid 1,2-dioleoyl-*sn-glycero*-3-phosphate (sodium salt) (18PA) cause β2-glycoprotein I (β2-GPI) to occupy the largest portion of the protein corona, where it interacts with THP-1 marcrophages and is delivered to the spleen.[121] Therefore, LNPs composed of the anionic helper lipid 18PA and ionizable lipids can be employed for treating pancreatic diseases through mRNA delivery facilitated by macrophages. Using the ionized lipids $306O_{i10}$, $514O_{6,10}$, lipid nanoparticles with $306O_{i10}$ showed the highest level of protein expression in the pancreas, whereas $514O_{6,10}$ showed no

specific delivery efficiency when administered IV but increased to 52% when administered IP.

mRNA expressed *via* particles made from ionized lipid modification showed the highest expression level after 6 h of incubation.[125] The expression of the delivered mRNA in the pancreas was sustained for more than 12 h, and it exhibited up to 137-fold higher expression compared to that in other organs. Additionally, the safety of mRNA-LNP administration was confirmed by H&E staining, which showed no tissue damage. This approach restored insulin production in pancreatic β-cells, demonstrating its potential for diabetes treatment.

Spleen targeted ionized lipids. The spleen is the largest lymphoid organ and plays a crucial role in regulating various aspects of the immune system, including antibody production, cytokine secretion, and activation of T cells. The spleen serves as a site for maturation and proliferation of B lymphocyte.[126] However, dysregulated B lymphocyte proliferation can lead to the development of lymphoma, which is responsible for 20 000 deaths in the United States annually. Additionally, B lymphocytes significantly impact autoimmune disorders, sclerosis, and cancer, underscoring the importance of regulating their activity for maintaining immune system balance.

To address these challenges, targeted drug delivery systems, such as liposomes and LNPs, are being developed for spleen-specific applications. For example, drug delivery systems coated with autoantibodies leverage Fc receptor-mediated phagocytosis to target the spleen. When particles are coated with immunoglobulin G (IgG), they are absorbed by FcγIIA receptors, enabling precise and effective delivery to the spleen.[127]

Modified ionized lipids, such as 1,2-dioleoyl-*sn-glycero*-3-phospho-L-serine (DOPS)[128] and OF-Deg-Lin,[129] both of which are anionic lipids,[120] are used when targeting the spleen. Anionic nanoparticles are generally known to have poor cellular uptake compared to cationic nanoparticles[120] due to the negative charge repulsion of anionic nanoparticles with the negatively charged cell membrane. Nevertheless, the aforementioned negative charge also serves a crucial function in facilitating precise and directed transportation to the spleen. Anionic nanoparticles have limited absorption by organs such as the liver or lungs, which typically demonstrate a strong propensity for nanoparticle uptake owing to their ionized characteristics.[120] In contrast, they have an affinity for selective accumulation and uptake inside the spleen. The spleen possesses specialized cells known as macrophages, which are responsible for scavenging and clearing foreign particles from the blood. Macrophages exhibit the ability to identify and phagocytose anionic nanoparticles, hence enhancing the targeted uptake of anionic nanoparticles and their accumulation in the spleen.[130] Specifically, OF-Deg-Lin-LNP, which has cationic ester bonds and is an anionic particle, is widely used. When OF-De-Lin was formulated into LNPs with DOPE, C14-PEG2000, cholesterol, and FLuc mRNA and subsequently injected IV into the tail vein of C57BL/6 mice, it showed fluorescence in the spleen (with more than 85% specificity) and induced more than 85% protein expression in the spleen.[129] Therefore, this approach holds significant promise for enhancing specific target delivery efficiency.

Future perspective

While oral administration of nanoparticles offers potential benefits such as improved patient compliance,[131,132] convenience,[133,134] and cost-effectiveness,[135] it may not always be superior when considering pharmacokinetic factors. Unlike intravenous (IV) injection, which provides a high area under the curve (AUC) and rapid drug delivery through direct access to the bloodstream,[136] oral administration faces significant challenges, including variable absorption influenced by food, gastric acid, and digestive enzymes. These factors can impact drug bioavailability and efficacy, making oral administration less predictable in pharmacokinetic terms. Additionally, drugs delivered orally often target multiple organs due to systemic circulation, which can complicate tissue-specific delivery.

To address these challenges, recent advancements have focused on leveraging ligand-modified LBNs to enhance tissue-specific targeting during oral delivery.[137] For example, aptamers have been conjugated with cholesterol in liposome formulations to target membranous cells (M cells) in the small intestine, utilizing receptor-mediated mechanisms to improve absorption.[138,139] While promising results have been observed in *ex vivo* studies, *in vivo* validation remains necessary to establish efficacy and reliability.

In addition, microneedle patch systems, which incorporate LBNs, have emerged as a transformative approach to overcoming barriers associated with drug delivery.[140,141] These minimally invasive systems enable precise delivery by bypassing the stratum corneum and providing direct access to the dermal microcirculation, thereby enhancing bioavailability and reducing first-pass metabolism. For instance, microneedle-mediated delivery of curcumin-loaded solid lipid nanoparticles has exhibited enhanced pharmacokinetics and therapeutic outcomes in neurodegenerative disease models, such as Parkinson's disease, by promoting sustained drug release and targeting efficiency.[142] Similarly, microneedles have been utilized to deliver lipid-based nanoparticles encapsulating compounds like rutin[143] and resveratrol,[144] demonstrating enhanced local bioavailability and reduced systemic side effects in models of obesity and neuroprotection. These systems have been shown to minimize patient discomfort and increase compliance by offering a convenient and effective alternative to conventional delivery routes. As research progresses, the optimization of microneedle design, nanoparticle composition, and formulation stability will be crucial for advancing these systems into clinical applications.

Further research is also required to optimize factors such as ligand density and specificity, which play a critical role in ensuring precise targeting and minimizing off-target effects. Additionally, integrating multi-omics approaches can provide insights into receptor expression patterns and tissue-specific absorption pathways, guiding the rational design of ligand-

modified nanoparticles. These strategies not only have the potential to overcome the limitations of oral delivery but also pave the way for the development of personalized and effective drug delivery systems tailored to individual patient needs.

Conclusion

In summary, advancements in LBNs have significantly improved drug absorption and delivery efficiency. Recent developments in LBNs, such as LNPs used in mRNA vaccines for COVID-19 by Pfizer-BioNTech and Moderna,[145] and liposomal formulations like Doxil®[146] and AmBisome®[147] for cancer and antifungal treatments, highlight their clinical and industrial relevance. Clinical trials for SLNs and nanoemulsions targeting neurodegenerative disorders, viral infections, and cancers further demonstrate their adaptability to various therapeutic needs. However, challenges remain, including the scalability of nanocarrier production, the long-term safety of repeated use, and off-target effects. These challenges must be addressed to ensure broader clinical adoption and efficacy.

The incorporation of ligands has emerged as a promising approach to enhance target specificity and improve drug delivery to specific organs or disease sites. Several types of ligands, including chemicals, saccharides, peptides, proteins, and ionized lipids, have demonstrated promise in facilitating targeted delivery through receptor- or pathway-mediated mechanisms. Notable examples include the incorporation of the GalNAc ligand in LNP systems, which has significantly improved the targeted delivery of drugs to the liver. Such advancements highlight the potential to discover new ligands based on organ-specific cellular absorption processes or the overexpression of disease-associated receptors. In the future, the ongoing investigation of ligand-based approaches and the development of novel combinations of multiple ligands will provide opportunities to attain greater efficacy in target-specific delivery. These advancements will play a crucial role in reducing adverse effects associated with nonspecific administration and transforming the management of diseases affecting various organs. Future work will focus on optimizing nanocarrier systems, addressing production challenges, and integrating ligand-based strategies for targeted therapies. These efforts aim to advance precision medicine by enabling therapeutics tailored to specific diseases or organs, improving outcomes and expanding treatment options.

Abbreviations

AF	Antibody fragment
AFM	Atomic force microscopy
Angptl3	Angiopoietin-like 3
APF	4-Aminophenyl-β-L-fucopyranoside
APM	4-Aminophenyl-α-D-mannopyranoside
apoA-I	Apolipoprotein A-I
ApoE	Apolipoprotein E
ASGPR	Asialoglycoprotein receptor
ASP	Aspirin
AUC	Area under the curve
BBB	Blood–brain barrier
Ce6	Chlorin 6
CIA-1	Cytosolic iron–sulfur protein assembly
CLD	Chronic liver disease
CMF	Cell membrane fragment
Cou-6	Coumarin 6
CXCR4	C–X–C chemokine receptor type 4
DDC	Diethyldithiocarbamate-copper Cu
DMG	1,2-Dimyristoyl-*rac-glycero*-3-methoxy
DODAP	1,2-Dioleoyl-3-dimethylammonium propane
DOPC	1,2-Dioleoyl-*sn-glycero*-3-phosphocholine
DOPE	1,2-Dioleoyl-*sn-glycero*-3-phosphoethanolamine
DOPS	1,2-Dioleoyl-*sn-glycero*-3-phospho-L-serine
DOTAP	Dioleoyl trimethylammonium propane
DPF	DSPE-PEG2000-APF
DPM	DSPE-PEG2000-APM
DPPC	1,2-Dipalmitoyl-*sn-glycero*-3-phosphocholine
DSPC	Distearoyl phosphatidylcholine
DTX	Docetaxel
EDC	*N*-(3-Dimethylaminopropyl)-*N*′-ethylcarbodiimide
EPR	Enhanced permeability and retention
FA	Ferulic acid
FLuc	Firefly luciferase
GalNAc	*N*-Acetylgalactosamine
HA	Hyaluronic acid
HBV	Hepatitis B virus
HCC	Hepatocellular carcinoma
HDL	High-density lipoprotein
HMVEC-Ls	Human lung microvascular endothelial cells
HPPH	2-[1-Hexyloxyethyl]-2-devinyl pyropheophorbide-α
HSC	Hepatic stellate cells
HUVEC	Human umbilical vein endothelial cell
IP	Intraperitoneal
IV	Intravenous
KC	Kupffer cells
LBN	Lipid-based nanomedicine
LDL-R	Low-density lipoprotein receptor
LNP	Lipid nanoparticle
LUV	Large unilamellar vesicle
MD	Maltodextrin
MD-CAP	Maltodextrin-OSA-modified starch capsule
MDR	Multidrug resistance
MD-SC	Maltodextrin-sodium caseinate
MFPL	Dual-ligand modified PEGylated liposome
MICA/B	MHC class I polypeptide-related sequence A and B
Nano-CaP	Nano-calcium phosphate
NHS	*N*-Hydroxysuccinimide
NKG2D	Natural killer group 2 member D
NR	Nicotinamide riboside
OSA	Octenyl succinic anhydride
o/w	Oil-in-water
PCX	Polymeric CXCR4 antagonist
PDT	Photodynamic therapy

PEG	Polyethylene glycol
PFOB	Perfluorooctylbromide
P-gp	P-glycoprotein
PTT	Photothermal therapy
RAET1H	Retinoic acid early transcripts-1
REV	Reverse-evaporation vesicle
ROS	Reactive oxygen species
SC	Subcutaneous
SENE	Spontaneous emulsification
SHM	Staggered herringbone micromixer
SLN	Solid lipid nanoparticle
SORT	Selective organ targeting
SR-B1	Scavenger receptor class B type 1
TDS	Thiamine disulfide system
TF	Anti-tissue factor
TLR	Toll-like receptor
TPGS	D-α-Tocopheryl polyethylene glycol-1000 succinate
TPGS	D-α-Tocopherol polyethylene glycol 1000 succinate
TSL	Thermosensitive liposome
USNE	Ultrasonication emulsification
Vtn	Vitronectin
w/o	Water-in-oil.

Author contributions

Y. Y., J. A., and H. J. K. contributed equally to writing the manuscript. H. Y. C. supervised and conceptualized the manuscript. Y. Y., J. A., and H. J. K. collected data. Y. Y. and J. A. contributed to the graphical illustration. H. Y. C. and H. K. C. revised the manuscript. All authors read and approved the final manuscript.

Data availability

No primary research results, software, or code have been included and no new data were generated or analysed as part of this review.

Conflicts of interest

There are no conflicts to declare.

Acknowledgements

This research was supported by the "National Institute of Health" research project (2023ER180101), the National Research Foundation of Korea (NRF) grant funded by the Korea government (MSIT) (RS-2023-00211360), and the Biomaterials Specialized Graduate Program through the Korea Environmental Industry and Technology Institute (KEITI) funded by the Ministry of Environment (MOE).

References

1 N. Dhiman, R. Awasthi, B. Sharma, H. Kharkwal and G. T. Kulkarni, *Front. Chem.*, 2021, **9**, 580118.
2 J. Lu, M. Liong, J. I. Zink and F. Tamanoi, *Small*, 2007, **3**, 1341–1346.
3 Y. Sahbaz, H. D. Williams, T. H. Nguyen, J. Saunders, L. Ford, S. A. Charman, P. J. Scammells and C. J. Porter, *Mol. Pharm.*, 2015, **12**, 1980–1991.
4 G. A. Koning and G. Storm, *Drug Discovery Today*, 2003, **8**, 482–483.
5 L. Azhar Shekoufeh Bahari and H. Hamishehkar, *Adv. Pharm. Bull.*, 2016, **6**, 143–151.
6 R. de Melo Barbosa, P. Severino, C. L. L. Finkler and E. de Paula, in *Materials for Biomedical Engineering*, ed. A.-M. Holban and A. M. Grumezescu, Elsevier, 2019, pp. 369–397, DOI: 10.1016/b978-0-12-818433-2.00011-x.
7 R. A. Maldonado, R. A. LaMothe, J. D. Ferrari, A. H. Zhang, R. J. Rossi, P. N. Kolte, A. P. Griset, C. O'Neil, D. H. Altreuter, E. Browning, L. Johnston, O. C. Farokhzad, R. Langer, D. W. Scott, U. H. von Andrian and T. K. Kishimoto, *Proc. Natl. Acad. Sci. U. S. A.*, 2015, **112**, E156–E165.
8 E. Blanco, H. Shen and M. Ferrari, *Nat. Biotechnol.*, 2015, **33**, 941–951.
9 J. Wu, *J. Pers. Med.*, 2021, **11**, 61.
10 Y. Okamoto, K. Taguchi, K. Yamasaki, M. Sakuragi, S. Kuroda and M. Otagiri, *J. Pharm. Sci.*, 2018, **107**, 436–445.
11 H. Maeda, H. Nakamura and J. Fang, *Adv. Drug Delivery Rev.*, 2013, **65**, 71–79.
12 J. Sprent and C. King, *Sci. Immunol.*, 2021, **6**, eabj9256.
13 E. Musielak, A. Feliczak-Guzik and I. Nowak, *Materials*, 2022, **15**, 682.
14 V. Francia, R. M. Schiffelers, P. R. Cullis and D. Witzigmann, *Bioconjugate Chem.*, 2020, **31**, 2046–2059.
15 A. Samad, Y. Sultana and M. Aqil, *Curr. Drug Delivery*, 2007, **4**, 297–305.
16 T. M. Allen and P. R. Cullis, *Adv. Drug Delivery Rev.*, 2013, **65**, 36–48.
17 R. H. Müller, K. Mäder and S. Gohla, *Eur. J. Pharm. Biopharm.*, 2000, **50**, 161–177.
18 W. Mehnert and K. Mäder, *Adv. Drug Delivery Rev.*, 2001, **47**, 165–196.
19 A. Akinc, A. Zumbuehl, M. Goldberg, E. S. Leshchiner, V. Busini, N. Hossain, S. A. Bacallado, D. N. Nguyen, J. Fuller, R. Alvarez, A. Borodovsky, T. Borland, R. Constien, A. de Fougerolles, J. R. Dorkin, J. K. Narayanannair, M. Jayaraman, M. John, V. Koteliansky, M. Manoharan, L. Nechev, J. Qin, T. Racie, D. Raitcheva, K. G. Rajeev, D. W. Y. Sah, J. Soutschek, I. Toudjarska, H.-P. Vornlocher, T. S. Zimmermann, R. Langer and D. G. Anderson, *Nat. Biotechnol.*, 2008, **26**, 561–569.
20 L. Kim, S. Jo, G.-J. Kim, K. H. Kim, S. E. Seo, E. Ryu, C. J. Shin, Y. K. Kim, J.-W. Choi and O. S. Kwon, *Nano Convergence*, 2023, **10**, 51.

21 D. E. Large, R. G. Abdelmessih, E. A. Fink and D. T. Auguste, *Adv. Drug Delivery Rev.*, 2021, **176**, 113851.
22 J. O. Eloy, M. Claro de Souza, R. Petrilli, J. P. Barcellos, R. J. Lee and J. M. Marchetti, *Colloids Surf., B*, 2014, **123**, 345–363.
23 J. Kotoucek, F. Hubatka, J. Masek, P. Kulich, K. Velinska, J. Bezdekova, M. Fojtikova, E. Bartheldyova, A. Tomeckova, J. Straska, D. Hrebik, S. Macaulay, I. Kratochvilova, M. Raska and J. Turanek, *Sci. Rep.*, 2020, **10**, 5595.
24 Y. Zhang, W. Fei, H. Zhang, Y. Zhou, L. Tian, J. Hao, Y. Yuan, W. Li and Y. Liu, *J. Inorg. Biochem.*, 2021, **225**, 111622.
25 X. Tan, X. Pang, M. Lei, M. Ma, F. Guo, J. Wang, M. Yu, F. Tan and N. Li, *Int. J. Pharm.*, 2016, **503**, 220–228.
26 L. Sercombe, T. Veerati, F. Moheimani, S. Y. Wu, A. K. Sood and S. Hua, *Front. Pharmacol.*, 2015, **6**, 286.
27 Y.-Q. Zhao, L.-J. Li, E.-F. Zhou, J.-Y. Wang, Y. Wang, L.-M. Guo and X.-X. Zhang, *Pharm. Fronts*, 2022, **04**, e43–e60.
28 M. J. Byun, J. Lim, S. N. Kim, D. H. Park, T. H. Kim, W. Park and C. G. Park, *BioChip J.*, 2022, **16**, 128–145.
29 D. Jung, S. Jang, D. Park, N. H. Bae, C. S. Han, S. Ryu, E.-K. Lim and K. G. Lee, *BioChip J.*, 2024, DOI: **10.1007/s13206-024-00182-y**.
30 J. Han, J. Lim, C.-P. J. Wang, J.-H. Han, H. E. Shin, S.-N. Kim, D. Jeong, S. H. Lee, B.-H. Chun, C. G. Park and W. Park, *Nano Convergence*, 2023, **10**, 36.
31 K. L. Swingle, A. G. Hamilton and M. J. Mitchell, *Trends Mol. Med.*, 2021, **27**, 616–617.
32 Y. Eygeris, S. Patel, A. Jozic and G. Sahay, *Nano Lett.*, 2020, **20**, 4543–4549.
33 K. J. Hassett, J. Higgins, A. Woods, B. Levy, Y. Xia, C. J. Hsiao, E. Acosta, O. Almarsson, M. J. Moore and L. A. Brito, *J. Controlled Release*, 2021, **335**, 237–246.
34 N. M. Belliveau, J. Huft, P. J. Lin, S. Chen, A. K. Leung, T. J. Leaver, A. W. Wild, J. B. Lee, R. J. Taylor, Y. K. Tam, C. L. Hansen and P. R. Cullis, *Mol. Ther. – Nucleic Acids*, 2012, **1**, e37.
35 D. Chen, K. T. Love, Y. Chen, A. A. Eltoukhy, C. Kastrup, G. Sahay, A. Jeon, Y. Dong, K. A. Whitehead and D. G. Anderson, *J. Am. Chem. Soc.*, 2012, **134**, 6948–6951.
36 S. J. Shepherd, D. Issadore and M. J. Mitchell, *Biomaterials*, 2021, **274**, 120826.
37 P. R. Cullis and M. J. Hope, *Mol. Ther.*, 2017, **25**, 1467–1475.
38 M. Viard, H. Reichard, B. A. Shapiro, F. A. Durrani, A. J. Marko, R. M. Watson, R. K. Pandey and A. Puri, *Nanomedicine*, 2018, **14**, 2295–2305.
39 M. Ripoll, E. Martin, M. Enot, O. Robbe, C. Rapisarda, M. C. Nicolai, A. Deliot, P. Tabeling, J. R. Authelin, M. Nakach and P. Wils, *Sci. Rep.*, 2022, **12**, 9483.
40 S. Novakowski, K. Jiang, G. Prakash and C. Kastrup, *Sci. Rep.*, 2019, **9**, 552.
41 M. Maeki, Y. Okada, S. Uno, K. Sugiura, Y. Suzuki, K. Okuda, Y. Sato, M. Ando, H. Yamazaki, M. Takeuchi, A. Ishida, H. Tani, H. Harashima and M. Tokeshi, *Appl. Mater. Today*, 2023, **31**, 101754.
42 E. Musielak, A. Feliczak-Guzik and I. Nowak, *Molecules*, 2022, **27**, 2202.
43 R.-A. Hernández-Esquivel, G. Navarro-Tovar, E. Zárate-Hernández and P. Aguirre-Bañuelos, in *Nanocomposite Materials for Biomedical and Energy Storage Applications*, ed. S. Ashutosh, IntechOpen, Rijeka, 2022, ch. 7, DOI: DOI: **10.5772/intechopen.102536**.
44 C. Schwarz, W. Mehnert, J. S. Lucks and R. H. Müller, *J. Controlled Release*, 1994, **30**, 83–96.
45 T.-T.-L. Nguyen and V.-A. Duong, *Encyclopedia*, 2022, **2**, 952–973.
46 T. Lin, P. Zhao, Y. Jiang, Y. Tang, H. Jin, Z. Pan, H. He, V. C. Yang and Y. Huang, *ACS Nano*, 2016, **10**, 9999–10012.
47 W. Mehnert and K. Mäder, *Adv. Drug Delivery Rev.*, 2012, **64**, 83–101.
48 I. Arduino, N. Depalo, F. Re, R. Dal Magro, A. Panniello, N. Margiotta, E. Fanizza, A. Lopalco, V. Laquintana, A. Cutrignelli, A. A. Lopedota, M. Franco and N. Denora, *Int. J. Pharm.*, 2020, **583**, 119351.
49 R. Kumar, A. Singh and N. Garg, *ACS Omega*, 2019, **4**, 13360–13370.
50 P. Ganesan and D. Narayanasamy, *Sustainable Chem. Pharm.*, 2017, **6**, 37–56.
51 R. Kanwar, M. Gradzielski and S. K. Mehta, *J. Phys. Chem. B*, 2018, **122**, 6837–6845.
52 N. M. Badawi, M. H. Teaima, K. M. El-Say, D. A. Attia, M. A. El-Nabarawi and M. M. Elmazar, *Int. J. Nanomed.*, 2018, **13**, 1313–1326.
53 A. Thakkar, S. Chenreddy, J. Wang and S. Prabhu, *Cell Biosci.*, 2015, **5**, 46.
54 H. Wang, L. Li, J. Ye, R. Wang, R. Wang, J. Hu, Y. Wang, W. Dong, X. Xia, Y. Yang, Y. Gao, L. Gao and Y. Liu, *Pharmaceutics*, 2020, **12**, 126.
55 J. M. Gutiérrez, C. González, A. Maestro, I. Solè, C. M. Pey and J. Nolla, *Curr. Opin. Colloid Interface Sci.*, 2008, **13**, 245–251.
56 R. K. Harwansh, R. Deshmukh and M. A. Rahman, *J. Drug Delivery Sci. Technol.*, 2019, **51**, 224–233.
57 J. Mujica-Alvarez, O. Gil-Castell, P. A. Barra, A. Ribes-Greus, R. Bustos, M. Faccini and S. Matiacevich, *Molecules*, 2020, **25**, 1357.
58 H. Y. Cho, T. Lee, J. Yoon, Z. Han, H. Rabie, K. B. Lee, W. W. Su and J. W. Choi, *ACS Appl. Mater. Interfaces*, 2018, **10**, 9301–9309.
59 K. Shanmugapriya, H. Kim, P. S. Saravana, B. S. Chun and H. W. Kang, *Colloids Surf., B*, 2018, **172**, 170–179.
60 B. Kang, M. K. Shin, S. Han, I. Oh, E. Kim, J. Park, H. Y. Son, T. Kang, J. Jung, Y. M. Huh, S. Haam and E. K. Lim, *BioChip J.*, 2022, **16**, 280–290.
61 I. Haizan, D. H. Park, M. Y. Choi, H. Lee and J. H. Choi, *BioChip J.*, 2023, **17**, 293–307.
62 S. K. Asrani, H. Devarbhavi, J. Eaton and P. S. Kamath, *J. Hepatol.*, 2019, **70**, 151–171.

63 Z. M. Younossi, G. Wong, Q. M. Anstee and L. Henry, *Clin. Gastroenterol. Hepatol.*, 2023, **21**, 1978–1991.
64 A. A. Madkhali, Z. T. Fadel, M. M. Aljiffry and M. M. Hassanain, *Saudi J. Gastroenterol.*, 2015, **21**, 11–17.
65 R. Bottger, G. Pauli, P. H. Chao, N. Al Fayez, L. Hohenwarter and S. D. Li, *Adv. Drug Delivery Rev.*, 2020, **154–155**, 79–101.
66 Y. Sato, H. Matsui, N. Yamamoto, R. Sato, T. Munakata, M. Kohara and H. Harashima, *J. Controlled Release*, 2017, **266**, 216–225.
67 S. Chen, Y. Y. Tam, P. J. Lin, A. K. Leung, Y. K. Tam and P. R. Cullis, *J. Controlled Release*, 2014, **196**, 106–112.
68 A. Ketkar-Atre, T. Struys, T. Dresselaers, M. Hodenius, I. Mannaerts, Y. Ni, I. Lambrichts, L. A. Van Grunsven, M. De Cuyper and U. Himmelreich, *Biomaterials*, 2014, **35**, 1015–1024.
69 P. Opanasopit, M. Sakai, M. Nishikawa, S. Kawakami, F. Yamashita and M. Hashida, *J. Controlled Release*, 2002, **80**, 283–294.
70 Z. Xu, L. Chen, W. Gu, Y. Gao, L. Lin, Z. Zhang, Y. Xi and Y. Li, *Biomaterials*, 2009, **30**, 226–232.
71 F. Jing, J. Li, D. Liu, C. Wang and Z. Sui, *Pharm. Biol.*, 2013, **51**, 643–649.
72 C. Lai, C. Li, X. Luo, M. Liu, X. Liu, L. Hu, L. Kang, Q. Qiu, Y. Deng and Y. Song, *Mol. Pharm.*, 2018, **15**, 2548–2558.
73 A. A. D'Souza and P. V. Devarajan, *J. Controlled Release*, 2015, **203**, 126–139.
74 Q. Zhang, X. Zhang, T. Chen, X. Wang, Y. Fu, Y. Jin, X. Sun, T. Gong and Z. Zhang, *Nanoscale*, 2015, **7**, 9298–9310.
75 T. Yamada, Y. Iwasaki, H. Tada, H. Iwabuki, M. K. Chuah, T. VandenDriessche, H. Fukuda, A. Kondo, M. Ueda, M. Seno, K. Tanizawa and S. Kuroda, *Nat. Biotechnol.*, 2003, **21**, 885–890.
76 K. J. Longmuir, S. M. Haynes, J. L. Baratta, N. Kasabwalla and R. T. Robertson, *Int. J. Pharm.*, 2009, **382**, 222–233.
77 S. I. Kim, D. Shin, T. H. Choi, J. C. Lee, G. J. Cheon, K. Y. Kim, M. Park and M. Kim, *Mol. Ther.*, 2007, **15**, 1145–1152.
78 P. Detampel, D. Witzigmann, S. Krahenbuhl and J. Huwyler, *J. Drug Targeting*, 2014, **22**, 232–241.
79 J. A. Kamps, H. W. Morselt, P. J. Swart, D. K. Meijer and G. L. Scherphof, *Proc. Natl. Acad. Sci. U. S. A.*, 1997, **94**, 11681–11685.
80 A. Garcia-Fernandez, F. Sancenon and R. Martinez-Manez, *Adv. Drug Delivery Rev.*, 2021, **177**, 113953.
81 G. V. Scagliotti, S. Novello and G. Selvaggi, *Ann. Oncol.*, 1999, **10**(Suppl 5), S83–S86.
82 M. Shirley, *Drugs*, 2019, **79**, 555–562.
83 E. Mendez-Enriquez and J. Hallgren, *Front. Immunol.*, 2019, **10**, 821.
84 H. Jin, M. Jeong, G. Lee, M. Kim, Y. Yoo, H. J. Kim, J. Cho, Y. S. Lee and H. Lee, *Adv. Funct. Mater.*, 2022, **33**, 2209432.
85 N. Li, Y. Mai, Q. Liu, G. Gou and J. Yang, *Drug Delivery Transl. Res.*, 2021, **11**, 131–141.
86 V. Sethuraman, K. Janakiraman, V. Krishnaswami, S. Natesan and R. Kandasamy, *Eur. J. Pharm. Sci.*, 2021, **158**, 105657.
87 K. Kusumoto, H. Akita, T. Ishitsuka, Y. Matsumoto, T. Nomoto, R. Furukawa, A. El-Sayed, H. Hatakeyama, K. Kajimoto, Y. Yamada, K. Kataoka and H. Harashima, *ACS Nano*, 2013, **7**, 7534–7541.
88 T. Ishitsuka, H. Akita and H. Harashima, *J. Controlled Release*, 2011, **154**, 77–83.
89 M. Motomura, H. Ichihara and Y. Matsumoto, *Bioorg. Med. Chem. Lett.*, 2018, **28**, 1161–1165.
90 C. Gao, K. Cheng, Y. Li, R. Gong, X. Zhao, G. Nie and H. Ren, *Nano Lett.*, 2022, **22**, 8801–8809.
91 F. U. Weiss, F. Laemmerhirt and M. M. Lerch, *Visc. Med.*, 2019, **35**, 73–81.
92 L. Ding, S. Tang, A. Yu, A. Wang, W. Tang, H. Jia and D. Oupicky, *ACS Appl. Mater. Interfaces*, 2022, **14**, 10015–10029.
93 S. Barman, I. Fatima, A. B. Singh and P. Dhawan, *Int. J. Mol. Sci.*, 2021, **22**, 4765.
94 P. W. Li, S. Luo, L. Y. Xiao, B. L. Tian, L. Wang, Z. R. Zhang and Y. C. Zeng, *Acta Pharmacol. Sin.*, 2019, **40**, 1448–1456.
95 M. Emamzadeh, M. Emamzadeh and G. Pasparakis, *ACS Appl. Bio Mater.*, 2019, **2**, 1298–1309.
96 A. Marengo, S. Forciniti, I. Dando, E. Dalla Pozza, B. Stella, N. Tsapis, N. Yagoubi, G. Fanelli, E. Fattal, C. Heeschen, M. Palmieri and S. Arpicco, *Biochim. Biophys. Acta, Gen. Subj.*, 2019, **1863**, 61–72.
97 S. Park, D. Kim, G. Wu, H. Jung, J. A. Park, H. J. Kwon and Y. Lee, *OncoTargets Ther.*, 2018, **11**, 8655–8672.
98 W. Yang, Q. Hu, Y. Xu, H. Liu and L. Zhong, *Mater. Sci. Eng., C*, 2018, **89**, 328–335.
99 P. Scheltens, B. De Strooper, M. Kivipelto, H. Holstege, G. Chetelat, C. E. Teunissen, J. Cummings and W. M. van der Flier, *Lancet*, 2021, **397**, 1577–1590.
100 M. Vaz and S. Silvestre, *Eur. J. Pharmacol.*, 2020, **887**, 173554.
101 J. Weller and A. Budson, *F1000Research*, 2018, **7**, F1000 Faculty Rev–1161.
102 B. R. Bloem, M. S. Okun and C. Klein, *Lancet*, 2021, **397**, 2284–2303.
103 F. N. Emamzadeh and A. Surguchov, *Front. Neurosci.*, 2018, **12**, 612.
104 J. M. Ellis and M. J. Fell, *Bioorg. Med. Chem. Lett.*, 2017, **27**, 4247–4255.
105 S. Sathornsumetee and J. N. Rich, *Anticancer Drugs*, 2006, **17**, 1003–1016.
106 P. Liu and C. Jiang, *Wiley Interdiscip. Rev.: Nanomed. Nanobiotechnol.*, 2022, **14**, e1818.
107 K. Ogawa, N. Kato, M. Yoshida, T. Hiu, T. Matsuo, S. Mizukami, D. Omata, R. Suzuki, K. Maruyama, H. Mukai and S. Kawakami, *J. Controlled Release*, 2022, **348**, 34–41.
108 H. Koepsell, *Pflugers Arch.*, 2020, **472**, 1299–1343.
109 X. Li, B. Qu, X. Jin, L. Hai and Y. Wu, *J. Drug Targeting*, 2014, **22**, 251–261.

110 K. Scherzinger-Laude, C. Schonherr, F. Lewrick, R. Suss, G. Francese and J. Rossler, *Int. J. Nanomed.*, 2013, **8**, 2197–2211.
111 F. Y. Yang, M. C. Teng, M. Lu, H. F. Liang, Y. R. Lee, C. C. Yen, M. L. Liang and T. T. Wong, *Int. J. Nanomed.*, 2012, **7**, 965–974.
112 N. Qi, S. Zhang, X. Zhou, W. Duan, D. Gao, J. Feng and A. Li, *J. Nanobiotechnol.*, 2021, **19**, 446.
113 S. Suryaprakash, Y. H. Lao, H. Y. Cho, M. Li, H. Y. Ji, D. Shao, H. Hu, C. H. Quek, D. Huang, R. L. Mintz, J. R. Bago, S. D. Hingtgen, K. B. Lee and K. W. Leong, *Nano Lett.*, 2019, **19**, 1701–1705.
114 H. Y. Cho, A. Mavi, S. D. Chueng, T. Pongkulapa, N. Pasquale, H. Rabie, J. Han, J. H. Kim, T. H. Kim, J. W. Choi and K. B. Lee, *ACS Appl. Mater. Interfaces*, 2019, **11**, 23909–23918.
115 R. G. R. Pinheiro, A. Granja, J. A. Loureiro, M. C. Pereira, M. Pinheiro, A. R. Neves and S. Reis, *Pharm. Res.*, 2020, **37**, 139.
116 Sonali, R. P. Singh, N. Singh, G. Sharma, M. R. Vijayakumar, B. Koch, S. Singh, U. Singh, D. Dash, B. L. Pandey and M. S. Muthu, *Drug Delivery*, 2016, **23**, 1261–1271.
117 Y. T. Ko, R. Bhattacharya and U. Bickel, *J. Controlled Release*, 2009, **133**, 230–237.
118 J. Liu, D. Gao, D. Hu, S. Lan, Y. Liu, H. Zheng, Z. Yuan and Z. Sheng, *Research*, 2023, **6**, 0030.
119 J. Li, J. Hu, D. Jin, H. Huo, N. Chen, J. Lin and X. Lu, *J. Nanobiotechnol.*, 2024, **22**, 672.
120 Q. Cheng, T. Wei, L. Farbiak, L. T. Johnson, S. A. Dilliard and D. J. Siegwart, *Nat. Nanotechnol.*, 2020, **15**, 313–320.
121 S. A. Dilliard, Q. Cheng and D. J. Siegwart, *Proc. Natl. Acad. Sci. U. S. A.*, 2021, **118**, e2109256118.
122 M. Qiu, Z. Glass, J. Chen, M. Haas, X. Jin, X. Zhao, X. Rui, Z. Ye, Y. Li, F. Zhang and Q. Xu, *Proc. Natl. Acad. Sci. U. S. A.*, 2021, **118**, e2020401118.
123 C. Loira-Pastoriza, K. Vanvarenberg, B. Ucakar, M. Machado Franco, A. Staub, M. Lemaire, J. C. Renauld and R. Vanbever, *Int. J. Pharm.*, 2021, **600**, 120504.
124 M. Qiu, Y. Tang, J. Chen, R. Muriph, Z. Ye, C. Huang, J. Evans, E. P. Henske and Q. Xu, *Proc. Natl. Acad. Sci. U. S. A.*, 2022, **119**, e2116271119.
125 J. R. Melamed, S. S. Yerneni, M. L. Arral, S. T. LoPresti, N. Chaudhary, A. Sehrawat, H. Muramatsu, M. G. Alameh, N. Pardi, D. Weissman, G. K. Gittes and K. A. Whitehead, *Sci. Adv.*, 2023, **9**, eade1444.
126 V. Bronte and M. J. Pittet, *Immunity*, 2013, **39**, 806–818.
127 R. Grozovsky, K. M. Hoffmeister and H. Falet, *Curr. Opin. Hematol.*, 2010, **17**, 585–589.
128 T. Kurosaki, C. Nakasone, Y. Kodama, K. Egashira, H. Harasawa, T. Muro, H. Nakagawa, T. Kitahara, N. Higuchi, T. Nakamura and H. Sasaki, *Biol. Pharm. Bull.*, 2015, **38**, 23–29.
129 O. S. Fenton, K. J. Kauffman, J. C. Kaczmarek, R. L. McClellan, S. Jhunjhunwala, M. W. Tibbitt, M. D. Zeng, E. A. Appel, J. R. Dorkin, F. F. Mir, J. H. Yang, M. A. Oberli, M. W. Heartlein, F. DeRosa, R. Langer and D. G. Anderson, *Adv. Mater.*, 2017, **29**, 1606944.
130 S. Q. Nagelkerke, C. W. Bruggeman, J. M. M. den Haan, E. P. J. Mul, T. K. van den Berg, R. van Bruggen and T. W. Kuijpers, *Blood Adv.*, 2018, **2**, 941–953.
131 J. F. Jin, L. L. Zhu, M. Chen, H. M. Xu, H. F. Wang, X. Q. Feng, X. P. Zhu and Q. Zhou, *Patient Prefer. Adherence*, 2015, **9**, 923–942.
132 J. Lou, H. Duan, Q. Qin, Z. Teng, F. Gan, X. Zhou and X. Zhou, *Pharmaceutics*, 2023, **15**, 484.
133 T. Malach, Z. Jerassy, B. Rudensky, Y. Schlesinger, E. Broide, O. Olsha, A. M. Yinnon and D. Raveh, *Am. J. Infect. Control*, 2006, **34**, 308–312.
134 A. M. Vargason, A. C. Anselmo and S. Mitragotri, *Nat. Biomed. Eng.*, 2021, **5**, 951–967.
135 M. S. Alqahtani, M. Kazi, M. A. Alsenaidy and M. Z. Ahmad, *Front. Pharmacol.*, 2021, **12**, 618411.
136 J. Cui, C. Li, W. Guo, Y. Li, C. Wang, L. Zhang, L. Zhang, Y. Hao and Y. Wang, *J. Controlled Release*, 2007, **118**, 204–215.
137 J. Zhu, Q. L. Wang, H. H. Li, H. Y. Zhang, Y. Zhu, E. Omari-Siaw, C. Y. Sun, Q. Y. Wei, W. W. Deng, J. N. Yu and X. M. Xu, *J. Drug Delivery Sci. Technol.*, 2018, **46**, 339–347.
138 Y. He, Y. Huang, H. Xu, X. Yang, N. Liu, Y. Xu, R. Ma, J. Zhai, Y. Ma and S. Guan, *Colloids Surf., B*, 2023, **222**, 113109.
139 T. T. T. Tran, A. Delgado and S. Jeong, *BioChip J.*, 2021, **15**, 109–122.
140 Y. Zuo, R. Sun, N. Del Piccolo and M. M. Stevens, *Nano Convergence*, 2024, **11**, 15.
141 A. D. Permana, M. A. S. b. Mahfud, M. Munir, A. Aries, A. R. Putra, A. Fikri, H. Setiawan, I. Mahendra, A. Rizaludin, A. Y. R. Aziz, Y. Y. Djabir, A. Arsyad, Y. Harahap, W. D. Saputri, R. Fajarwati and N. Darmawan, *ACS Appl. Mater. Interfaces*, 2024, **16**, 68388–68406.
142 A. Prabhu, J. Jose, L. Kumar, S. Salwa, M. Vijay Kumar and S. M. Nabavi, *AAPS PharmSciTech*, 2022, **23**, 49.
143 Z. Li, S. Liang, H. Sun, C. Bao and Y. Li, *ACS Appl. Mater. Interfaces*, 2023, **15**, 54294–54303.
144 A. Bandiwadekar, J. Jose, G. Gopan, V. Augustin, H. Ashtekar and K. B. Khot, *Drug Delivery Transl. Res.*, 2024, **15**, 1043–1073.
145 D. Hallas, R. Spratling and J. Fletcher, *J. Pediatr. Health Care*, 2021, **35**, 443–448.
146 X. Wu, Y. Zhu, W. Huang, J. Li, B. Zhang, Z. Li and X. Yang, *Adv. Sci.*, 2018, **5**, 1700859.
147 V. Heinemann, D. Bosse, U. Jehn, B. Kähny, K. Wachholz, A. Debus, P. Scholz, H. J. Kolb and W. Wilmanns, *Antimicrob. Agents Chemother.*, 1997, **41**, 1275–1280.